Deuteron breakup induced by protons and neutrons

H. Kumpf, J. Mösner, K. Möller, and G. Schmidt

Central Institute for Nuclear Research, Rossendorf, German Democratic Republic
Fiz. Elem. Chastits At. Yadra 9, 412–452 (March–April 1978)

Theoretical and experimental investigations on deuteron breakup induced by protons and neutrons with energy up to 50 MeV are reviewed. A description is given of the nonrelativistic three-particle kinematics, the experimental techniques, and the basic theoretical equations for describing scattering in a three-particle system. The most important experimental results of recent years and their theoretical interpretation are discussed. It is shown that at the present time a good understanding has been achieved of the *Nd* breakup mechanism and that one can with good accuracy extract the low-energy parameters of two-particle scattering, in particular, the *nn* scattering length; however, despite the good agreement between the experimental data and the theoretical calculations it is impossible to obtain reliable quantitative data on the off-shell behavior of nuclear forces and three-body forces.

PACS numbers: 25.10.+s, 21.40.+d

INTRODUCTION

Significant successes have been achieved in the last two decades in the study of the three-nucleon system. Faddeev's pioneering work[1] was followed by many calculations of the scattering states of three nucleons for the *NN* interaction.

Fundamental questions were posed by Mitra,[2] Amado,[3] Lovelace,[4] Sitenko and Kharchenko,[5] Weinberg,[6] and Alt *et al.*[7] The rapid development of computing techniques made it possible to carry out practical calculations[8-13] and compare them with experimental data.

Significant progress has also been achieved in experimental investigations of *pd* and *nd* scattering. Improved detectors and measuring techniques, and also the modern methods of data evaluation, made possible kinematically complete experiments with sufficient effectiveness.

The growing interest in problems of the three-nucleon system was reflected in many publications, and also conferences (Brela, 1976; Birmingham, 1969; Los Angeles, 1972; Quebec, 1974; Delhi, 1976) and symposia (Liblice, 1974; Tübingen, 1975; Vlieland, 1976; Uppsala, 1977; Potsdam, 1977).

This interest is explained above all by the fact that in nuclear physics there is a tendency to reduce the complicated properties of a system of nucleons to the interaction between tow nucleons. Although it is impossible to assert at the moment that this problem can be solved for heavy nuclei, the description of the three-nucleon system can be a first step in this direction. Here, we also have questions relating to the completeness of our knowledge of the *NN* interaction, especially off the energy shell, and also the importance of many-particle forces. The efforts of many physicists (theoreticians and experimentalists) in recent years have been directed toward the solution of these two problems.

The reaction $^2\mathrm{H}(n, 2n)p$ plays a key role in investigations of the neutron-neutron interaction, being of great importance in connection with the charge symmetry of nuclear forces.

There have been a number of reviews devoted to this subject. In Refs. 14–17 the Faddeev equations and methods for solving them are discussed; in Ref. 18, the connection between the two- and three-nucleon problems. A review of deuteron breakup induced by nucleons is contained in Ref. 19; data on nuclei with $A = 3$ in Ref. 20; an analysis of the angular distributions in the case of deuteron breakup, in Refs. 19 and 21. Review talks at conferences are given in Refs. 22 and 23, and invesitgations on the *nn* scattering length are compared in Ref. 24.

In the present paper, we review the experimental investigations on deuteron breakup by nucleons and we analyze them. We discuss mainly the results of the last three years. The energy range is limited to about 50 MeV of the incident nucleon in the laboratory system. Bound states and the breakup of the deuteron by other particles are not considered.

Section 1 contains an introduction to the kinematics and the experimental methods of kinematically complete experiments. The exposition is limited to nonrelativistic kinematics and detection of charged particles. In incomplete measurements, the integration with respect to one of the coordinates results in a partial loss of information. Therefore, such experiments are not considered.

In Sec. 2, we present scattering theory for three particles for the *NN* interaction, and also the common model representations and certain principles of numerical solution of the three-body problem for separable potentials.

In Sec. 3, we discuss the results of some experimental and theoretical papers that have appeared since 1974. Here, particular attention is devoted to comparing theory and experiment and studying the off-shell behavior of the *NN* interaction.

At the end, we consider the present state of the problem and make some predictions for the future.

 0090-4759/78/020170-18$02.80

1. KINEMATIC RELATIONS AND EXPERIMENTAL METHODS IN DEUTERON BREAKUP INVESTIGATIONS

General Kinematic Conditions. In a three-particle reaction, the laws of energy and momentum conservation in the laboratory system take the form

$$E_0+Q=E_1+E_2+E_3; \tag{1}$$

$$\mathbf{p}_0=\mathbf{p}_1+\mathbf{p}_2+\mathbf{p}_3. \tag{2}$$

The kinematics of such a reaction is determined by the nine momentum components of the three final particles. Using the four equations (1) and (2), the problem of a kinematically complete measurement reduces to determining the differential cross section as a function of five variables that satisfy the following condition:

$$(1+m_1/m_3)\,E_1+(1+m_2/m_3)\,E_2+(2/m_3)\,(\sqrt{m_1m_2E_1E_2}\,(\cos(1,2)-\sqrt{m_0m_1E_0E_1}\cos\theta_1-\sqrt{m_0m_2E_0E_2}\cos\theta_2)-(1-m_0/m_3)\,E_0-Q=0;$$
$$\cos(1,2)=\cos\theta_1\cos\theta_2+\sin\theta_1\sin\theta_2\cos(\varphi_1-\varphi_2), \tag{3}$$

where E_0 and m_0 are the energy and mass of the projectile; Q is the Q of the reaction; θ_1 and θ_2 are polar angles; φ_1 and φ_2 are the azimuthal angles; and E_1 and E_2 are the kinetic energies of particles 1 and 2. Equation (3) describes an ellipse[25] in the coordinate system with $\sqrt{E}_1$ and $\sqrt{E}_2$ as axes. In the center-of-mass system,

$$E_{\text{tot}}^{\text{cm}}=E_1^{\text{cm}}+E_2^{\text{cm}}+E_3^{\text{cm}}, \tag{4}$$

where $E_{\text{tot}}^{\text{cm}}=(1-m_0/M)E_0+Q$ is the total energy; $E_1^{\text{cm}}, E_2^{\text{cm}}, E_3^{\text{cm}}$ are the cms kinetic energies of the three particles.

We introduce Jacobi momentum coordinates:

$$\mathbf{p}_{1\text{-}23}=\mu_{1\text{-}23}\,[\mathbf{p}_1/m_1-(\mathbf{p}_2+\mathbf{p}_3)/(m_2+m_3)]=\mathbf{p}_1-(m_1/M)\,\mathbf{p}_0; \tag{5}$$

$$\mathbf{p}_{2\text{-}3}=\mu_{2\text{-}3}\,(\mathbf{p}_2/m_2-\mathbf{p}_3/m_3), \tag{6}$$

where $\mu_{1\text{-}23}=m_1(m_2+m_3)/M$; $\mu_{2\text{-}3}=m_2m_3/(m_2+m_3)$; $M=m_1+m_2+m_3$. We obtain the expressions for $\mathbf{p}_{2\text{-}13}$, $\mathbf{p}_{3\text{-}12}$, $\mathbf{p}_{1\text{-}3}$, and $\mathbf{p}_{1\text{-}2}$ by an appropriate change of the indices. Then the relative energies can be expressed as follows:

$$E_{1\text{-}23}=\mathbf{p}_{1\text{-}23}^2/2\mu_{1\text{-}23}; \tag{7}$$

$$E_{2\text{-}3}=\mathbf{p}_{2\text{-}3}^2/2\mu_{2\text{-}3}=E_{\text{tot}}^{\text{cm}}-ME_1^{\text{cm}}/(m_2+m_3), \tag{8}$$

and the energy conservation law is represented in the form

$$E_{\text{tot}}^{\text{cm}}=E_{1\text{-}23}+E_{2\text{-}3}=(m_2+m_3)\,E_{2\text{-}3}/M+(m_1+m_3)\,E_{1\text{-}3}/M+(m_1+m_2)\,E_{1\text{-}2}/M. \tag{9}$$

If, following Dalitz,[26, 172] we introduce the reduced energies ε:

$$\varepsilon_1\equiv ME_1^{\text{cm}}/(m_2+m_3)\,E_{\text{tot}}^{\text{cm}}=1-E_{2\text{-}3}/E_{\text{tot}}^{\text{cm}} \tag{10}$$

and similarly for ε_2 and ε_3, then (9) takes the form

$$(m_2+m_3)\,\varepsilon_1+(m_1+m_3)\,\varepsilon_2+(m_1+m_2)\,\varepsilon_3=M. \tag{11}$$

With each particle we associate one side in a triangle;

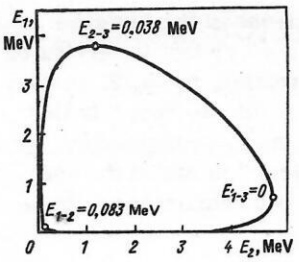

FIG. 1. Connection between the energies E_1 and E_2, in the laboratory system, of the two observed particles for a kinematically complete experiment. The points of minimal relative energy between the particle pairs are indicated.

then the ε will correspond to the distances of a point from these sides if the angles α are calculated in accordance with the formula

$$\tan(\alpha_1/2)=(m_2m_3/m_1M)^{1/2} \tag{12}$$

(similarly for α_2 and α_3).

For the case of deuteron breakup induced by protons, Fig. 1 shows as an example the kinematic curve in accordance with Eq. (3) for $E_0=8.5$ MeV, $\theta_1=35°$, $\theta_2=48.72°$, and $\varphi_1-\varphi_2=180°$. The same thing in the Dalitz plot is shown in Fig. 2. Here, the end points of the curve correspond to the intersections of the curve with the E_1 axis in the preceding graph. The points of minimal relative energy are indicated.

Separation of Regions of Phase Space. If polarization phenomena are not considered, the differential cross section depends on four variables, which form the phase space. In practice, it is always necessary to restrict oneself to certain regions of the phase space. In what follows, we shall give kinematic conditions for certain regions that have particular importance for measurements of deuteron breakup.

In the following equations, $Q=-2.2246$ MeV is the deuteron binding energy; $\mu=1$ and 2 if the incident particles are nucleons and deuterons, respectively.

1. Regions of constant relative energy (for example, $E_{1\text{-}2}=\text{const}$). It follows from (8) that $E_3^{\text{cm}}=\text{const}$. A particular subregion is determined by the condition of quasifree scattering (QFS).

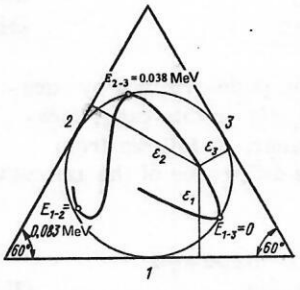

FIG. 2. Image of the kinematic curve of Fig. 1 in the Dalitz plot.

This means that one of the nucleons in the deuteron remains fixed, for example, $p_3 = 0$, or that it carries on with unchanged velocity and direction, $p_3 = p_0/2$, in the case of an incident deuteron. It follows from this that the reaction is coplanar, i.e., the three momentum vectors lie in one plane. Particle 3 is called the spectator. The polar angles of the two remaining particles are related by

$$\cos\theta_2 = (\sqrt{E_0/\mu} - \sqrt{E_1}\cos\theta_1)/\sqrt{E_0/\mu - E_1 + Q}; \quad (13)$$

$$\sqrt{E_1} = (1/2)\,[\sqrt{E_0/\mu}\cos\theta_1 \pm \sqrt{(E_0/\mu)\cos^2\theta_1 + 2Q}]. \quad (14)$$

The relative energy is $E_{1-2} = E_0/2\mu + Q$, from which it follows that $\varepsilon_3 = E_0/(4E_0 + 6\mu Q)$. In the symmetric case $\theta_1 = \theta_2 = \theta$, i.e., $E_1 = E_2 = E$. Then

$$\cos\theta = \sqrt{E_0/2\,(E_0 + \mu Q)}; \quad (15)$$

$$E = (E_0/\mu + Q)/2. \quad (16)$$

Another particular subregion is that corresponding to final-state interaction (FSI) at zero relative energy, for example, $E_{2-3} = 0$. In this case, $E_1^{cm} = 2E_{tot}^{cm}/3$ and $\varepsilon_1 = 1$. Particles 2 and 3 move in the same direction with equal velocities: $p_2 = p_3$; the reaction is coplanar. The polar angles are related by the conditions

$$\cos\theta_2 = (\sqrt{\mu E_0} - \sqrt{E_1}\cos\theta_1)/\sqrt{2\,(E_0 + Q - E_1)}; \quad (17)$$

$$\sqrt{E_1} = \tfrac{1}{3}\,[\sqrt{\mu E_0}\cos\theta_1 \pm \sqrt{\mu E_0\cos^2\theta_1 + (6 - 3\mu)\,E_0 + 6Q}]. \quad (18)$$

The cms production angle is determined by the equation

$$\sin\theta_1^{cm} = \sqrt{E_1}\sin\theta_1/\sqrt{2\,(2E_0/3\mu + Q)/3}. \quad (19)$$

2. Regions in which two relative energies are equal: $E_{1-2} = E_{2-3}$. A particular subregion is the collinear case. Particle 3 is at rest in the final state in the center-of-mass system: $p_3^{cm} = 0$, i.e., $p_3 = p_0/3$. The reaction is again coplanar. The following relations hold:

$$\cos\theta_2 = (2/3)\,\sqrt{\mu E_0} - \sqrt{E_1}\cos\theta_1)/\sqrt{(9 - \mu)\,E_0/9 + Q - E_1}; \quad (20)$$

$$\sqrt{E_1} = (1/3)\,[\sqrt{\mu E_0}\cos\theta_1 \pm \sqrt{\mu E_0\cos^2\theta_1 + (9 - 5\mu)\,E_0/2 + 9Q/2}]; \quad (21)$$

$$\sin\theta_1^{cm} = \sqrt{2E_1/(2E_0/3\mu + Q)}\sin\theta_1. \quad (22)$$

In the symmetric case, $\theta_1 = \theta_2 = \theta (E_1 = E_2 = E)$ and the equations simplify:

$$\cos\theta = \sqrt{2\mu E_0/[(9 - \mu)\,E_0 + 9Q]}; \quad (23)$$

$$E = [(9 - \mu)\,E_0/9 + Q]/2; \quad \theta_1^{cm} = \pi/2. \quad (24)$$

Another particular subregion is determined by equality of the polar angles: $\theta_1 = \theta_2 = \theta$; in this case, however, the reaction is not coplanar. It follows from $E_{1-2} = E_{2-3}$ that $E_1 = E_2 = E$. The difference of the azimuthal angles $\varphi_2 - \varphi_1$ satisfies

$$\cos(\varphi_2 - \varphi_1) = [2\sqrt{\mu E_0 E}\cos\theta + (1 - \mu)\,E_0/2 + Q/2 - E\,(2 + \cos^2\theta)]/E\sin^2\theta. \quad (25)$$

The energy is calculated in accordance with

$$\sqrt{E} = (1/3)\,[\sqrt{\mu E_0}\cos\theta \pm \sqrt{\mu E_0\cos^2\theta + (6 - 3\mu)\,E_0 + 6\,(Q - E_{2-3})}]. \quad (26)$$

3. Region in which two relative energies are equal and constant (for example, $E_{1-3} = E_{2-3} = \text{const}$). This region is contained in the more general case 2. From Eq. (9) we then find that E_{1-2} is also constant:

$$E_{1-3} = \sqrt{\mu E_0 E_2}\cos\theta_2 - 3E_2/2 + Q + (1 - \mu/2)\,E_0; \quad (27)$$

$$E_{1-3} = E_{2-3} = \sqrt{\mu E_0 E_1}\cos\theta_1 - 3E_1/2 + Q + (1 - \mu/2)\,E_0 = \text{const}. \quad (28)$$

One can, for example, specify θ_1 and E_1 and represent the differential cross section as a function of E_3. In this case, $E_{2-3} = E_{1-3}$ is obtained from (28), E_2 is calculated from energy conservation, θ_2 from (27), and $(\varphi_2 - \varphi_1)$ from (3).

Another possible choice is the symmetric case: $\theta_1 = \theta_2 = \theta$ and $E_{1-2} = E_{1-3} = E_{2-3} = E_{tot}^{cm}/2$. The differential cross section can be represented as a function of E_3, and the value of $E_1 (E_1 = E_2)$ follows from energy conservation. From (27) or (28) we obtain $\theta_1 (\theta_1 = \theta_2)$, and from (25) the difference $(\varphi_2 - \varphi_1)$.

The last subregion, the so-called symmetric point, is a special case. It is determined by the condition $\theta_1 = \theta_2 = \theta_3 = \theta$, from which it follows that $E_1 = E_2 = E_3 = (E_0 + Q)/3$. From momentum conservation,

$$\cos\theta = \sqrt{\mu E_0/3\,(E_0 + Q)}; \quad \varphi_2 - \varphi_1 = 2\pi/3; \quad (29)$$

the cms momenta are perpendicular to p_0.

In Eqs. (14), (18), (21), and (26), the minus sign can occur only if the total expression remains positive.

For clarity, it is helpful to represent the positions of these regions in the Dalitz plot (Fig. 3). At each point of the Dalitz disk, except for the three points of interaction in the final state $\varepsilon = 1$, two variables can be specified in addition. A uniform distribution of events in phase space also gives a uniform filling of the Dalitz disk.

Experiments. As we have already said, a three-particle reaction is completely determined if five kinematic variables are measured. This means that one must detect at least two particles in coincidence. A frequently used arrangement for measuring two protons in coin-

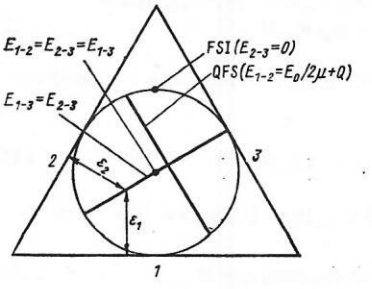

FIG. 3. Image of kinematically distinguished regions of the phase space in the Dalitz plot.

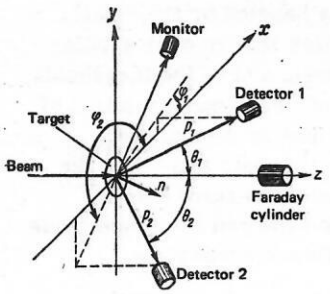

FIG. 4. Arrangement for measurements of deuteron breakup.

cidence is shown in Fig. 4. A beam of protons or neutrons strikes a hydrogenous target and is absorbed in the Faraday cylinder. The protons are detected by two detectors set up at variable angles θ_1, φ_1 and θ_2, φ_2 and cover the solid angles $\Delta\Omega_1$ and $\Delta\Omega_2$. To these, a monitor to count elastic pd scattering is usually added. The target and detectors are in a scattering chamber at a vacuum of 10^{-5}-10^{-6} torr. Such arrangements have been described by various authors.[27-38] Arrangements for detecting a neutron and proton in coincidence are considered in Refs. 39–46. Neutrons in the ingoing channel were used in Refs. 47–56.

The further discussion will be limited to measurements of two protons.

To achieve sufficient angular resolution, the particle beam is focused into a spot of a few square millimeters. The targets are either gaseous or polyethylene ($0.1 - 1\ mg/cm^2$); the preparation of such foils is described in Ref. 57, for example. The particle flux is usually 50–500 nA. Since a polyethylene foil melts or is rapidly depleted of hydrogen at such a current density,[58] it is advisable to rotate the target[59] or move it in some other way.[60] Surface barrier detectors are the ones most frequently used. They ensure an energy resolution of 10–20 keV and a time resolution of about 1 nsec. By cooling and by using high voltages one can improve these data somewhat (see, for example, Ref. 61).

Circular diaphragms whose edges are treated in a special way are usually placed in front of the detectors. Their diameters are measured with an error ~0.01 mm. They determine the solid angles $\Delta\Omega_1$ and $\Delta\Omega_2$, which lie in the interval 10^{-2}–10^{-4} sr.

If the incident particles are deuterons, it is frequently necessary to discriminate the particle species. One uses either the standard $\Delta E - E$ method[41,44,62-64] at proton energies above 1.5 MeV, or the time-of-flight method.[56] The latter method of course presupposes a pulsed beam.

The detectors are mounted on booms or disks. The angle scale is calibrated and tested in different ways. Besides optical alignment, one can, for example, use elastic scattering on gold to test the symmetry with respect to the beam and the values of the polar angles. A proven method is to determine the "intersection angles" of the reactions $^2H(p,d)p$ and $^{12}C(p,p')^{12}C^*$ (4.433 MeV). The polar angles at which the energies of elastically scattered deuterons and inelastically scattered protons are equal depends only on the beam energy and can be measured with accuracy ~±0.05°.[66] The reaction $^{12}C(p,p')^{12}C^*$ can also be used to calibrate the energy of the detector. With an electrostatic generator, one can achieve an uncertainty of ±2 keV in the energy calibration.

To calibrate the time ratios in the system of two detectors one can use the reaction $^1H(p,2p)$. For $\theta_1 = \theta_2 = 45°$ and equal distances of the detectors from the target the two protons hit the detectors simultaneously. In this way one can find the zero point of the time axis. The time scale is usually measured by calibrated delay cables.

If the charged particles are measured by semiconductor detectors, it is usually assumed that the detection efficiency is close to unity. Various people have found that this is not always true (see, for example, Ref. 67). Therefore, before and after a series of experiments it is necessary to test the detector efficiency by means of a flux of particles of known intensity or by the comparison method.

To make best use of the accelerator time, it is advantageous to use more than two detectors in coincidence. A very complicated experiment with 64 detector telescopes was set up on the synchrocyclotron at Amsterdam. This system covers 13% of the complete solid angle.[68] The distribution of the E detectors in a checkerboard array with 88 fields gives an angular resolution of 1°. A system of 192 detectors is used at the Texas A& M University.[69] The detectors consist of plastic NE-102 scintillators and RCA 4517 photomultipliers. The angular resolution is of order three degrees and the 192 detectors together cover 3.5% of the total solid angle.

At the tandem generator at Uppsala an experiment was set up with six detectors and controlled electronics in the CAMAC system. According to the data given in Ref. 70, the efficiency is increased by about 10 times compared with an experiment with two detectors.

The investigation of polarization phenomena in deuteron breakup experiments requires a special measuring technique, which is not discussed here. As yet, very few measurements of this kind have been made.[71-73] In them, polarized beams of protons or deuterons were used and the asymmetry of the cross section for definite combinations of angles or the analyzing power $A_y(\theta)$ in the region of the np interaction in the final state were investigated.

Electronics for Data Evaluation. Figure 5 shows the circuit of a simple scheme with two detectors for an unpulsed beam. Each preamplifier gives time and spectroscopic signals. The time signals with rise time ~10 nsec are amplified in the fast amplifiers, shaped in the shapers, and they trigger or stop the time-to-amplitude converter. The stop signal is delayed by 50–100 nsec. The output signal of the converter is proportional to the time interval between the two time signals. It is encoded in an ADC. The spectroscopic signals

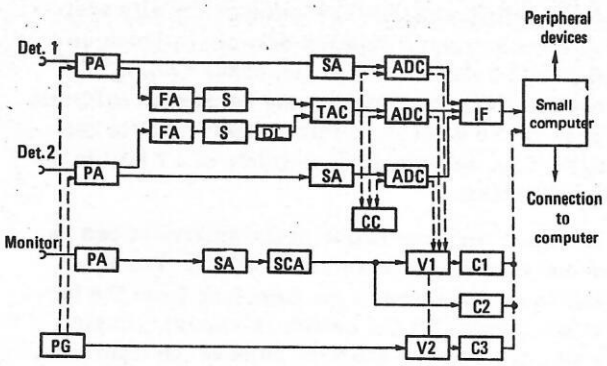

FIG. 5. Electronics for deuteron breakup measurements: PA, preamplifier; FA, fast amplifier; *SA*, spectroscopic amplifier; S, discriminator and shaper; DL, delay line; TAC, time-to-amplitude converter; ADC, analog-to-digital converter; CC, coincidence circuit; IF, interface; SCA, single-channel analyzer; V, gate; C, counter; PG, pulse generator.

(rise time ~1 μsec) are amplified in the spectroscopic amplifiers and are also encoded. The three converters are connected to a coincidence circuit. They are triggered only when the signals arrive in an interval of 1 μsec. The three digital signals (or words) are combined in the input device into the total word and fed to a small computer. It stores the total words first in a buffer device. In the case of so-called off-line processing the data are then put onto magnetic tape or some other storage. After the measurement, the collected events are processed in the computer and sorted into spectra. This method is also called event storing. For off-line processing, the events are processed during the time of the measurement after the buffer has been filled. To avoid interrupting the measurements during the processing time, newly arriving events are collected in a second buffer (ping-pong regime). The pulses of the monitor are also amplified. A single-channel analyzer separates the line of elastically scattered protons or deuterons, and the counters C1 and C2 measure the intensity. To allow for the dead time of the converters, the monitor signals can be fed through the gate V1, which is shut during the dead time of one of the converters.

To test the readiness and stability of the system, it is advisable to feed control pulses of frequency 0.1–1 Hz from a pulse generator to the preamplifier inputs. They pass through the blocks like real signals and accumulate in a free channel of the spectrum. After a definite interval, for example, after each filling of the buffer, the computer compares the number of control pulses in the spectrum with the contents of counter C3. To eliminate control pulses that arise during the dead time of one of the converters, there must be a second gate, shut synchronously with V1, in front of the counter C3. It is advisable to realize such methods of automatic control in the CAMAC system.

By means of this arrangement, one can process a counting rate ~5.10^3 pulse/sec in individual channels without particular difficulty. For usual values of the solid angles, one then obtains not more than 10 events/sec, which can also be readily handled by the small computer. Higher counting rates lead to ever greater uncertainties because of displacement of the thresholds, displacement and broadening of lines, superposition of pulses, increase in the dead time, and incorrect matching of the time and spectroscopic signals in the coincidence circuit of the three converters. In this case, additional measures are required to reduce these effects or to take them into account accurately.

In the event evaluation in the computer, the first test is to find out if the two protons were emitted simultaneously from the target. Since the computer knows the energy of the two protons, it can take into account the time-of-flight difference, and also the amplitude-dependent delay of the shaper. Noise leads to random displacements in time. All events within a certain time interval are deemed to be true. To avoid the loss of true events, the width of the interval must exceed the half-width Δt due to the noise by at least a factor four. The value of Δt depends on the rise time t_A of the pulses from the detector, the rise time t_{AF} of the fast amplifiers, and the minimal energy E_{min} of the protons in the spectrum[74]:

$$\Delta t \sim \sqrt{t_{AF}+t_A^2/t_{AF}}/E_{min} \qquad (30)$$

All true coincidences are plotted in a two-dimensional spectrum with E_1 and E_2 as axes. All events that lie outside this interval but within another definite interval are either rejected or sorted into a second spectrum, and subsequently into the spectrum of random coincidences.[38]

Representation of Measured Data. As a result of the measurements, we obtain a distribution of events between discrete channels which is spread out to both sides of the central kinematic curve by the finite angu-

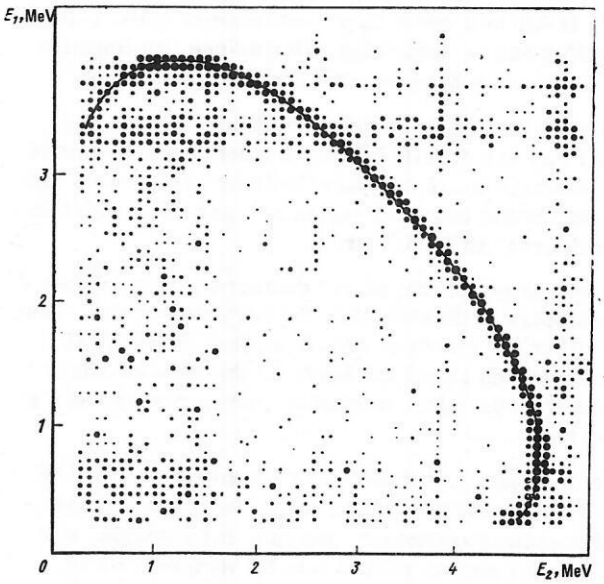

FIG. 6. Measured spectrum of *pd* breakup with kinematic curve. The areas of the points correspond to the number of events collected in the given channel. One event corresponds to the smallest point; 64 to the largest.

lar and energy resolutions. As an example, we give the results of measurements (Fig. 6) with initial data corresponding to the curve in Fig. 1. The intensity of the spots corresponds to the number of events in the channel. To compare the measured distribution with theoretical calculations, one must either calculate the theoretical cross section for each channel with allowance for the experimental resolutions (convolution), or reduce the measured two-dimensional spectrum to a one-dimensional distribution. The former can be realized by, for example, the Monte Carlo method.[75] In practice, the latter path is usually chosen since it reduces the volume of data.

The simplest thing is to project the distribution onto one of the energy axes. The result of projection is

$$d\sigma^3/d\Omega_1\, d\Omega_2\, dE_1 = N_i/\Delta\Omega_1\Delta\Omega_2\Delta E_{1i} N_E N_T. \quad (31)$$

Here, N_i is the number of pulses in the interval ΔE_{1i}; N_E is the number of incident particles; N_T is the number of target atoms per 1 cm^2. A shortcoming of this method is that it does not apply in the region in which the tangent is perpendicular to the energy axis, and also that the representation is two-valued on account of the quadratic dependence of $E_1 - E_2$. For this reason, one usually uses a projection of the spectrum onto the central kinematic curve. Various methods are known (see, for example, Refs. 66, 76, 77, and 143).

Suppose S is the arc length. Then

$$d^3\sigma/d\Omega_1\, d\Omega_2\, dS = (d^3\sigma/d\Omega_1\, d\Omega_2\, dE_1)\, dE_1/dS = (d^3\sigma/d\Omega_1\, d\Omega_2\, dE_1)/\sqrt{1+(dE_2/dE_1)^2}. \quad (32)$$

The product $N_E N_T$ in (31) is needed to calculate the absolute value of the cross section. As already noted, it is usually determined by means of the monitor which measures the elastic scattering:

$$d\sigma_{el}/d\Omega = N_M/\Delta\Omega_M N_E N_T, \quad (33)$$

where N_M is the number of elastically scattered protons or deuterons; $\Delta\Omega_M$ is the solid angle of the monitor. The elastic differential cross section of the reaction ^{2}H$(p,p)^2$H is known to within a few percent for the necessary energies and angles.[20] Equation (31) then takes the form

$$d^3\sigma/d\Omega_1\, d\Omega_2\, dE_1 = (N_i\Delta\Omega_M/\Delta\Omega_1\Delta\Omega_2\Delta E_{1i} N_M)\, d\sigma_{el}/d\Omega. \quad (34)$$

If the second detector is used simultaneously as monitor, then $\Delta\Omega_1$ in (34) cancels with $\Delta\Omega_2$.

As a measure of the agreement between the reduced experimental and theoretical values one usually adopts[28] the quantity χ^2:

$$\chi^2 = \sum_i \frac{(\sigma_i^{exp} - \sigma_i^{theor})^2}{(\Delta\sigma_i^{exp})^2}. \quad (35)$$

Here, σ_i^{exp} and σ_i^{theor} are, respectively, the experimental and theoretical values in channel i, and $\Delta\sigma_i^{exp}$ is the error in the measurement of σ_i^{exp}. If statistical errors predominate, $(\Delta\sigma_i^{exp})^2 \sim \sigma_i^{exp}$. In the case of comparison with the distribution obtained by the Monte Carlo method,[1,55]

$$\chi^2 = \frac{1}{N}\sum_i \frac{(\sigma_i^{exp} - N\sigma_i^{theor})^2}{(\Delta\sigma_i^{exp})^2 + (\Delta\sigma_i^{theor})^2}; \qquad N = \sum_i \sigma_i^{exp} \Big/ \sum_i \sigma_i^{theor}. \quad (36)$$

Here, $\Delta\sigma_i^{theor}$ is the statistical error due to the finite number of samplings.

2. BASIC THEORY OF DEUTERON BREAKUP

Theory of Two-Particle Scattering. For the theoretical description of *Nd* scattering, we first review some of the basic theory of two-particle scattering.

If a potential v acts between the nucleons, the scattering operator t is determined by the integral equation

$$t(z_2) = v + v g_0(z_2)\, t(z_2), \quad z_2 = E_2 + i0. \quad (37)$$

Here, E_2 is the cms energy of the two-particle system; $g_0(z_2) = (z_2 - h_0)^{-1}$ is the Green's operator; h_0 is the Hamiltonian of the free motion. In the momentum representation, (37) takes the form

$$\langle \mathbf{k}'|t|\mathbf{k}\rangle = \langle \mathbf{k}'|v|\mathbf{k}\rangle + \int \frac{d^3k''}{(2\pi)^3} \frac{\langle \mathbf{k}'|v|\mathbf{k}''\rangle\langle \mathbf{k}''|t|\mathbf{k}\rangle}{(z_2 - k''^2)}. \quad (38)$$

The normalization condition is $\langle \mathbf{k}'|\mathbf{k}\rangle = (2\pi)^3\delta(\mathbf{k}'-\mathbf{k})$. It is known from general scattering theory that the matrix element $\langle \mathbf{k}'|t|\mathbf{k}\rangle$ describes the transition from the state $|\mathbf{k}\rangle$ to the state $|\mathbf{k}'\rangle$ accompanying scattering with a potential v between the particles. The cross section is

$$d\sigma(E_2, \vartheta)/d\Omega = (1/16\pi^2)\,|\langle \mathbf{k}'|t(z_2)|\mathbf{k}\rangle|^2;\ k^2 = k'^2 = E_2;\ \cos\vartheta = \mathbf{k}'\cdot\mathbf{k}/k'k. \quad (39)$$

The condition $\mathbf{k}'^2 = \mathbf{k}^2 = E_2$ expresses the energy conservation law. It can be seen from (39) that for two-particle scattering only the diagonal elements of t with respect to k and k' are needed. These are the on-shell matrix elements. The remainder are the off-shell elements. Sometimes, one also uses half-off-shell elements. For them $\mathbf{k}'^2 = E_2 \neq \mathbf{k}^2$ or $\mathbf{k}'^2 \neq E_2 = \mathbf{k}^2$.

One of the fundamental questions of nuclear physics is the determination of nuclear forces. For known scattering operator t, one can find the operator v by inverting Eq. (37). However, in accordance with (39) it is impossible to determine t completely from two-particle scattering data; one can determine only the diagonal elements. Therefore, it is impossible to find the potential completely from experiments on two-particle scattering. To obtain a unique potential, one must augment the two-particle data. Gelfand and Levitan[79] showed that the potential becomes unique if one also requires it to be local. Another way of obtaining additional information about the potential is to investigate scattering in systems with more than two particles.

Naturally, one first turns to a three-particle system.

In the following section, we shall show that the off-shell matrix elements really do occur in the equations for three-particle scattering. The extraction of information about off-shell behavior from three-particle experiments is made harder by the occurring of these elements in integral form in the equations. In addition, it is difficult to separate many-particle effects, for example, three-particle forces. The clarification of these problems is the most important aim of *Nd* breakup investigations. The off-shell properties of the matrix t can be studied by comparing the spectra of three-particle scattering for different potentials that are equivalent as regards the phase shifts. Such potentials differ only off-shell, and lead to the same phase shifts

of two-particle scattering and the same energies of bound states, if such exist. Sets of phase-shift-equivalent potentials can be obtained from a certain given potential by phase-shift-equivalent transformations.[12,13,80] Because of the difficulties of solving integral equations of three-particle scattering for complicated potentials, systematic investigations of this kind have only just begun.[13,81]

In most calculations of *Nd* scattering, potentials that describe the behavior at only low energies, even on the energy shell, are used. If one is working at low energies, this approximation is justified to some extent because the three-particle equations contain the two-particle t matrix only for $-\infty < E_2 \leq E_3$ [see (49)]. Frequently, the two-particle interaction is characterized merely by the phase shift[82,83]:

$$k \cot \delta_0 = -1/a + r_0 k^2/2 - ck^4/(1+dk^2), \tag{40}$$

where a is the scattering length and r_0 the effective range.

There are two special forms of the potential v that play an important role in what follows: local and separable. A local potential is one of the form

$$\langle \mathbf{r}' | v | \mathbf{r} \rangle = v(\mathbf{r})\,\delta(\mathbf{r}'-\mathbf{r}). \tag{41}$$

A separable potential of rank N can be represented in the form

$$v = \sum_{i=1}^{N} \lambda_i |\chi_i\rangle\langle\chi_i|; \tag{42a}$$

$$\langle \mathbf{k}' | v | \mathbf{k} \rangle = \sum_{i=1}^{N} \lambda_i g_i(\mathbf{k}')\, g_i(\mathbf{k}), \tag{42b}$$

where we have introduced the form factors $g_i(\mathbf{k}) \equiv \langle \mathbf{k} | \chi_i \rangle$.

Rigorous Three-Particle Theory. Calculations of scattering in a three-particle system are based on Faddeev's equations.[1,84] These are a system of integral equations that is equivalent to a Schrödinger equation with unique boundary conditions. For the scattering state $|\psi_i\rangle$ of *Nd* breakup, the Faddeev equations have the form

$$|\psi_i\rangle = |\psi^{(1)}\rangle + |\psi^{(2)}\rangle + |\psi^{(3)}\rangle; \tag{43a}$$

$$\begin{pmatrix} |\psi^{(1)}\rangle \\ |\psi^{(2)}\rangle \\ |\psi^{(3)}\rangle \end{pmatrix} = \begin{pmatrix} |\phi_{Nd}\rangle \\ 0 \\ 0 \end{pmatrix} + G_0(z_3) \begin{pmatrix} 0 & T_{23}(z_3) & T_{23}(z_3) \\ T_{31}(z_3) & 0 & T_{31}(z_3) \\ T_{12}(z_3) & T_{12}(z_3) & 0 \end{pmatrix} \begin{pmatrix} |\psi^{(1)}\rangle \\ |\psi^{(2)}\rangle \\ |\psi^{(3)}\rangle \end{pmatrix},$$

$$z_3 = E_3 + i0. \tag{43b}$$

Here, $G_0(z_3)$ is the Green's operator of free motion of the three particles. The operators $T_{ij}(z_3)$ are determined by the integral equations

$$T_{ij}(z) = v_{ij} + v_{ij} G_0(z)\, T_{ij}(z), \tag{43c}$$

where v_{ij} is the potential between particles i and j.

The state of the ingoing channel $|\phi_{Nd}\rangle$ (deuteron and free nucleon) satisfies the equation

$$(H_0 + v_{23})|\phi_{Nd}\rangle = E_3 |\phi_{Nd}\rangle. \tag{43d}$$

The matrix element of the transition to three free particles is expressed in terms of

$$T_{fi} = \langle \phi_f(E) | v_{23} + v_{31} + v_{12} | \psi_i(E_3) \rangle \quad E \to E_3; \tag{44a}$$

$$T_{fi} = (E_3 - E)\langle \phi_f(E) | \psi_i(E_3) \rangle. \quad E \to E_3. \tag{44b}$$

Here, we have used the Schrödinger equation:

$$\left.\begin{aligned} (H_0 + v_{23} + v_{31} + v_{12})|\psi_i(E_3)\rangle = E_3 |\psi_i(E_3)\rangle; \\ H_0 |\phi_f(E)\rangle = E |\phi_f(E)\rangle. \end{aligned}\right\} \tag{45}$$

There are a number of alternative formulations of the equations of three-particle scattering; the most important of them are given in Refs. 4, 5, 7, and 85. The Faddeev equations of the *Nd* system with allowance for spin, isospin, and antisymmetrization were first given in Ref. 5. A review of the quantum-mechanical theory of a three-particle system can be found in Ref. 17.

Solution of the Faddeev Equations. We introduce Jacobi momentum coordinates in the form

$$\left.\begin{aligned} \mathbf{p} = (\mathbf{k}_1 + \mathbf{k}_2 + \mathbf{k}_3)/\sqrt{6}; \\ \mathbf{p}_1 = (\mathbf{k}_2 - \mathbf{k}_3)/2; \\ \mathbf{q}_1 = (\mathbf{k}_2 + 2\mathbf{k}_3 - 2\mathbf{k}_1)/2\sqrt{3}, \end{aligned}\right\} \tag{46}$$

where $\mathbf{k}_1, \mathbf{k}_2, \mathbf{k}_3$ are the cms momenta of the three particles in a system of units with $\hbar = m = 1$. Alongside the momenta $\mathbf{p}_1$ and $\mathbf{q}_1$, the coordinates $\mathbf{p}_2, \mathbf{q}_2$ and $\mathbf{p}_3, \mathbf{q}_3$, which are obtained from (46) by substitution of the indices, are also used in the Faddeev equations. After the center-of-mass motion has been eliminated, the three-particle wave function still depends on six variables. A further simplification is achieved by an expansion with respect to the angular momentum.[15,86-89] Usually, this expansion is made with respect to the quantum numbers of the total orbital angular momentum L, its z component M, the orbital angular momentum l of one pair, and the angular momentum λ of the third particle with respect to the chosen pair. As a result, we obtain an infinite coupled system of integral equations for the partial-wave functions, these depending on two continuous variables. There are infinitely many equations since for given L there are infinitely many combinations of l and λ coupled to L. In the important case of a short-range potential, the equations contain only the lowest values of l and the system becomes finite. The overwhelming majority of investigations into *Nd* breakup has been restricted to the value $l = 0$. Even in this case the solution of the two-dimensional integral equations on modern computers is a complicated problem. Attempts were made to solve the problem directly[90] and indirectly for local potentials by means of the Padé approximation[11] or the quasiparticle method.[7,91] The calculated scattering cross sections usually agree well with the experiment even under the restriction $l = 0$ in the case of two-body interaction. However, to calculate the polarization it is necessary to take into account tensor forces and larger values of l. As yet, polarization has been considered almost exclusively for elastic *Nd* scattering.[92,93] There are still very few measurements of polarization in *Nd* breakup,[72,73] and the theoretical results are limited.[94]

In the calculation of *Nd* breakup, the separable model occupies a central position. It is obtained from the Faddeev equations by using a separable potential. The resulting one-dimensional integral equation can be solved on a computer with comparative ease, especially if a potential with only one term is used. Of the large number of calculations using the separable model (or the Amado model) we mention only a few: Refs. 2, 3, 5, 8, 9, 13, 15, 94, and 95.

Here, we consider the equations for a separable potential in a form such as they were given in Ref. 13. The equations take into account the spin, isospin, antisymmetrization, and potential of rank N in the form

$$v_i = \sum_{\mu=1}^{N} \lambda_{i\mu} |\chi_{i\mu}\rangle \langle\chi_{i\mu}|; \quad i = \begin{cases} 1\ {}^3S_1\ np \\ 2\ {}^1S_0\ np \\ 3\ {}^1S_0\ nn, np. \end{cases} \tag{47}$$

The subscript i labels the spin–isospin state of the two-particle system. As can be seen from (47), the two-particle interaction is assumed to be charge dependent. For the potential (47), the two-particle t matrix takes the form

$$t_i(z) = \sum_{\mu,\nu=1}^{N} |\chi_{i\mu}\rangle \tau^i_{\mu\nu}(z) \langle\chi_{i\nu}|. \tag{48a}$$

Here, the $\tau^i_{\mu\nu}(z)$ are determined by the equations

$$\left.\begin{aligned} &\tau^i_{\mu\nu} = \lambda_{i\mu} (A_i^{-1})_{\mu\nu}; \\ &(A_i)_{\mu\nu} = \delta_{\mu\nu} - \lambda_{i\nu} \int \frac{d^3k}{(2\pi)^3} \frac{g_{i\mu}(k)\, g_{i\nu}(k)}{(z - k^2)}. \end{aligned}\right\} \tag{48b}$$

Under these conditions, the Faddeev equations can be written in the form

$$X^S_{j\lambda 11}(\mathbf{q}', q; z_3) = \Lambda^S_{j1} V_{j\lambda 11}(\mathbf{q}', q; z_3) + \sum_{k=1}^{3} \sum_{\mu,\nu=1}^{N} \Lambda^S_{jk} \int d^3q'' V_{j\lambda k\mu}(\mathbf{q}', \mathbf{q}''; z_3) \tau^k_{\mu\nu}(z_3 - q''^2) X^S_{k\nu 11}(\mathbf{q}'', q; z_3). \tag{49}$$

Here, the indices j and k determine the spin–isospin state; λ, μ, and ν are individual separable terms. The coupling matrices Λ^s_{jk} have the from (S is the total spin of the three-particle system)

$$\Lambda^{3/2}_{jk} = -\delta_{j1}\ \delta_{k1}; \Lambda^{1/2}_{jk} = \begin{pmatrix} 1/2 & -1/2 & -1 \\ -3/2 & -1/2 & 1 \\ -3/2 & 1/2 & 0 \end{pmatrix}. \tag{50a}$$

For charged-independent forces, we obtain only two coupled equations ($j, k = 1, 2$) with coupling matrices

$$\Lambda^{3/2}_{jk} = -\delta_{j1}\ \delta_{k1}; \Lambda^{1/2}_{jk} = \frac{1}{2} \begin{pmatrix} 1 & -3 \\ -3 & 1 \end{pmatrix}. \tag{50b}$$

Frequently, charge dependence is taken into account only by the so-called hybrid approximation.[95] In this case, the system (49) for X^S is solved as for charge-independent forces. As the spin-singlet two-particle interaction one considers either the singlet np interaction[95] or a modified interaction with averaged scattering parameters $a_S^{-1} = 2a_{np}^{-1}/3 + a_{pp}^{-1}/3$ and $r_0 = 2r_{np}/3 + r_{pp}/3$ (Ref. 9). As will be shown later [see (53)], the total breakup amplitude contains not only χ^S but also the factors g and τ. In them, the charge dependence is taken into account exactly.

In (49), the $V_{j\lambda k\mu}(\mathbf{q}', q; z_3)$ are determined by the equation

$$V_{j\lambda k\mu}(\mathbf{q}', q; z) = \frac{g_{j\lambda}\left(\sqrt{4(q - q'/2)^2}\ 3\right) g_{k\mu}\left(\sqrt{4(q'/2 - q')^2}/3\right)}{3z/4 - q^2 - q'^2 - qq'} \tag{51a}$$

with form factor

$$g_{j\lambda}(p) = \langle p | \chi_{j\lambda}\rangle. \tag{51b}$$

To solve (49), it is necessary to expand the total amplitude with respect to the partial-wave amplitudes:

$$X^S_{j\lambda 11}(\mathbf{q}', q; z) = \sum_{L=0}^{\infty} (2L+1) X^S_{j\lambda 11, L}(q', q; z) P_L(\hat{q}'\hat{q}). \tag{52}$$

From this we can readily obtain a system of integral equations for the amplitudes $X^S_{j\lambda 11, L}$. For calculation of the Nd breakup cross section, it is necessary that

$$T^S_k(\mathbf{p}', \mathbf{q}') = \sum_{\mu\nu} c g_{k\mu}(p') \tau^k_{\mu\nu}(z_3 - q'^2) X^S_{k\nu 11}(\mathbf{q}', q; z_3). \tag{53}$$

The constant c in (53) arises when we express the deuteron wave function $|\varphi_d\rangle$ in the ingoing channel in terms of the form factor $|\chi_{11}\rangle$. We have the relation

$$|\varphi_d\rangle = c g_0(E_d) |\chi_{11}\rangle, \tag{54}$$

where $g_0(E_d)$ is the Green's function of the two-particle system at the binding energy E_d. From (53), we obtain the square of the total matrix element of the breakup process:

$$|T|^2 = (2/3)\,|T^{3/2}|^2 + (1/3)|T_t^{1/2}|^2 + (1/3)\,|T_s^{1/2}|^2; \tag{55}$$

$$\left.\begin{aligned} &T^{3/2} = T_1^{3/2}(\mathbf{p}_1, q_1) - T_1^{3/2}(\mathbf{p}_2, q_2); \\ &T_t^{1/2} = \frac{1}{2}[T_1^{1/2}(\mathbf{p}_1, q_1) - T_1^{1/2}(\mathbf{p}_2, q_2) + T_2^{1/2}(\mathbf{p}_1, q_1) - T_2^{1/2}(\mathbf{p}_2, q_2)]; \\ &T_s^{1/2} = \frac{2}{\sqrt{3}}\Big[T_3^{1/2}(\mathbf{p}_3, q_3) + \frac{1}{4} T_2^{1/2}(\mathbf{p}_1, q_1) + \frac{1}{4} T_2^{1/2}(\mathbf{p}_2, q_2) - \frac{3}{4} T_1^{1/2}(\mathbf{p}_1, q_1) - \frac{3}{4} T_1^{1/2}(\mathbf{p}_2, q_2)\Big]. \end{aligned}\right\} \tag{56}$$

The weight factors in (56) arise because of the antisymmetrization, and the factors in (55) from the summation over the spins in the outgoing channel and averaging over the spins in the ingoing channel. In (56), particles 1 and 2 are assumed to be identical.

The expression we have obtained applies to kinematically complete experiments. For incomplete experiments, it is necessary to integrate with respect to the unobserved variable. The cross section of a complete experiment has the form

$$\frac{d^5\sigma}{d\Omega_1\, d\Omega_2\, dE_1} = \frac{(2\pi)^{10}}{\hbar v_0} \left(\frac{\hbar^2}{m}\right)^{9/2} \left(\frac{\sqrt{3}}{2}\right)^6 \rho |T|^2, \tag{57}$$

with the phase density

$$\rho = (2\pi)^{-3} (m/\hbar^2)^3 k_1 k_2 [2 - (\mathbf{k}_0 - \mathbf{k}_1)\, k_2/k_2^2]^{-1}. \tag{58}$$

Here, v_0 and $\mathbf{k}_0$ are the velocity and momentum of the incident particle; $\mathbf{k}_1$ and $\mathbf{k}_2$ are the laboratory momenta of the detected particles. The cross section has the dimensions $F^2 \cdot sr^{-2} \cdot MeV^{-1}$. Although the use of separable potentials simplifies the treatment of the three-particle problem, the numerical solution of the system (49) is seriously complicated by the presence in the kernel of the integral equation of a pole above the two-particle decay threshold, $E_3 > E_d$, and logarithmic singularities above the breakup threshold $E_3 > {}_0$. It is only in recent years that a number of methods have been developed that make it possible to solve the system on a computer.

In the first calculations made in the separable model, the method of contour deformation was used.[8,9,95,96] In it, the contour of integration is displaced into the complex plane of the variables of integration in such a way that the distances to the singularities become sufficiently great for one to be able to use the classical formulas of numerical integration. This method guarantees sufficient accuracy of the results; a shortcoming of it is that for each form factor one must first investigate its analytic behavior in the complex plane of the argument. For this reason, methods of numerical integration along the real axis were developed. They allow any form factors, which can even be given in tabulated form. Here, we have the method of moments,[92,97] the modi-

fied method of moments,[98] and the method proposed in Ref. 99. All these approaches are based on a splitting of the kernel of the integral equation into singular and nonsingular terms. The nonsingular terms are replaced by interpolation polynomials, and the remaining integrals with respect to the singular terms are solved analytically. The results obtained by the different numerical methods differ from one another by about 2% or less,[13,100] so that at the present time one can hardly doubt the correctness of the numerical results of the separable model.

We shall also mention some other possibilities for analyzing three-particle scattering, although the majority of numerical results have hitherto been obtained from the Faddeev equation and, in particular, from the separable model.

It was shown in Ref. 101 that the Faddeev equations can be transformed into an integrodifferential equation in coordinate space. In Refs. 102 and 103, the boundary conditions needed to solve this modified Faddeev equation were found. The method was used to calculate the bound state of three particles and the *Nd* scattering phase shifts.[104-105] An important role is here also played by the boundary-condition model (BCM).[106-109] In this model, the two-particle potential at short distances is replaced by boundary conditions at a certain radius. The boundary conditions and the external potential are chosen in such a way that the experimental two-particle phase shifts are reproduced. The energy-dependent boundary conditions can simulate different off-shell behavior of the potential. It is asserted in Ref. 108 on the basis of the boundary-condition model that one cannot extract information about off-shell nuclear forces from deuteron breakup that is not already contained in the *Nd* doublet scattering length. However, others have not confirmed this conclusion.[12,13,110] The advantage of the boundary-condition model is that it can be readily generalized for the relativistic case and that it leads to one-dimensional integral equations, like the separable model. In contrast to the latter, there is a large discrepancy between the BCM results obtained by different authors, even for the bound states.[111]

Simple Models. As we have already said, exact calculations on the basis of the Faddeev equations have been made only in recent years. Before that, the spectra from deuteron breakup were explained almost exclusively on the basis of two simple models-the Migdal-Watson model[112,113] and the so-called spectator model. The success of the models is due to the fact that the structure of the three-particle spectra is basically determined by two simple mechanisms: the so-called final-state interaction (FSI) and the quasifree scattering (QFS) of two of the participating particles. In the FSI mechanism, it is assumed that the breakup takes place

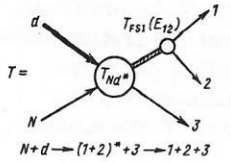

FIG. 7. Diagram of final-state interaction.

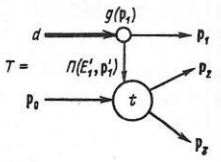

FIG. 8. Diagram of quasi-free scattering.

in two stages. In the exit channel, a separate particle and an intermediate system of two particles is first formed. In the second stage, the intermediate system breaks up into two particles (Fig. 7). If the FSI mechanism is to be realized, the two-particle forces must be capable of forming the intermediate state. In the case of *NN* interaction, this condition is satisfied as the result of the virtual level $^1S_0$. As Migdal[113] showed, for low relative energies E_{12} between particles 1 and 2 the form of the three-particle spectrum is determined by the $^1S_0$ level [the factor $T_{FSI}(E_{12})$]:

$$|T|^2 = |T_{Nd^*}|^2 |T_{FSI}(E_{12})|^2, \tag{59a}$$

where

$$|T_{FSI}(E_{12})|^2 \approx (E_{12}+E_s)^{-1} \approx (k^2+k^2\cot^2\delta_0)^{-1} \approx \{k^2+(-1/a_s+r_{0s}k^2/2)^2\}^{-1} \tag{59b}$$

where $E_{12}=k^2$. Here, the following relations between the energy E_s of the virtual level and the singlet scattering parameters a_s and r_{0s} are used:

$$E_s=\alpha^2; \quad \alpha=a_s^{-1}+r_{0s}\alpha^2/2; \quad E_s=-67\,\text{keV}. \tag{59c}$$

The last equation in (59b) follows from the effective-range formula (40). The factor $|T_{Nd^*}|^2$ in (59a) can be assumed to vary slowly for low relative energies E_{12}, so that in this region the form of the spectrum is determined by the factor T_{FSI}.

The second mechanism, quasifree scattering, is obtained by assuming that the incident nucleon is scattered on only one of the two nucleons in the deuteron, no momentum being transferred to the other one, which is a "spectator". Because of the low deuteron binding energy, this model gives a good explanation of the process even at low energies. The quantitive description of quasifree scattering[114,115] takes into account the momentum distribution of the nucleon in the deuteron in accordance with the diagram in Fig. 8. Here, $\mathbf{p}_0, \mathbf{p}_1, \mathbf{p}_2, \mathbf{p}_3$ are the laboratory momenta of the ingoing and outgoing particles. Energy and momentum conservation give $E_1'=-E_d-p_1^2/2m$ and $\mathbf{p}_1'=-\mathbf{p}_1$. The process takes place in two stages. First, the deuteron, which is described by the vertex part $g(\mathbf{p}_1)$, decays virtually in a state of rest, and then the incident particle is scattered on one of the two particles. This process is described by the two-particle scattering matrix t. The propagator is

$$\Pi(E_1', p_1') = E_1' - p_1'^2/2m = (-E_d - p_1^2/2m) - p_1^2/2m = -E_d - p_1^2/m; \tag{60}$$

$$T = g(\mathbf{p}_1)\langle \mathbf{p}_2, \mathbf{p}_3 | t(z-3p_1^2/4m) | \mathbf{p}_0, -\mathbf{p}\rangle/\Pi(E_1', p_1'); \tag{61a}$$

$$T = \varphi_d(\mathbf{p}_1)\langle \mathbf{p}_2, \mathbf{p}_3 | t(z-3p_1^2/4m) | \mathbf{p}_0, -\mathbf{p}_1\rangle. \tag{61b}$$

Here, $\varphi_d(\mathbf{p}_1)$ is the deuteron wave function:

$$\varphi_d(\mathbf{p}_1) = -g(\mathbf{p}_1)/(E_d+p_1^2/m) = -g(\mathbf{p}_1)/(E_d+2E_1). \tag{62}$$

It can be seen from the expression for φ_d that the matrix element has a peak at $E_1=0$, i.e., when particle 1

remains at rest (is a spectator). It is assumed that $g(p_1)$ does not vary too strongly in this region.

The simple impulse approximation (SIA) presupposes a constant matrix element along the kinematic curve, so that the form of the spectrum is described by just the wave function $\varphi_d(k)$. Modifications of the simple impulse approximation are worth mentioning: SIA with sharp cutoff[116] and SIA with smooth cutoff.[117]

Allowance for Coulomb Interaction. An important problem in calculations of deuteron breakup induced by protons is the allowance for Coulomb forces. This is a question of considerable practical importance since *pd* scattering experiments are made much more often than *nd* ones, being simpler and more accurate. However, to obtain reliable data on nuclear forces from *pd* experiments one must know the influence of the Coulomb interaction on the *pd* breakup spectra. Methods for allowing for the electromagnetic interaction in the three-nucleon problem are reviewed in Ref. 118.

If the solution of the Faddeev equations for realistic potentials is difficult even without the Coulomb interaction, with it the problem can be imagined. The Faddeev equations cannot be used in their original form because of the r^{-1} dependence of the electrostatic potential. In Refs. 119 and 120, the Faddeev equations were modified by changing the kernel of the integral equations in such a way as to make it completely continuous. This can be achieved by, for example, eliminating the purely Coulomb term or the most obstreperous singularities from the kernel; the Green's function and inhomogeneous term are modified accordingly.

Another formulation of the three-particle problem with Coulomb interaction is derived from the already mentioned integrodifferential equation[101] using the boundary conditions with Coulomb interaction given in Ref. 121.

In Ref. 122, the problem of the Coulomb interaction is solved by the quasiparticle method. As Alt's investigations showed, the quasiparticle method, as a method which works well for local potentials, is well suited to take account the Coulomb interaction. For a separable nuclear potential of rank 1, Alt[222] calculated the $^4\delta_0$ phase shift of *pd* scattering both below and above the breakup threshold.

The breakup spectra have not yet been calculated with rigorous allowance for the electrostatic forces. In modern computer programs, which are based almost exclusively on Amado's model, the Coulomb forces are usually taken into account only in the final-state interaction. This is done in such a way that the energy distribution for uncharged particles is replaced by the corresponding distribution for charged particles.[123, 124] The final-state interaction for charged particles was investigated as early as 1955 by Migdal.[113] The factor $|T_{FSI}|^2$ in Eq. (59) is replaced in the case of two protons by

$$|T_{FSI}|^2 \sim C_0^4/[k^2C_0^4+(-1/a_{pp}+r_{0pp}k^2/2-h(\eta)/R)^2], \quad (63)$$

where an effective-range expansion is used for the charged particles (see, for example, Ref. 82):

$$C_0^2 k\cot\delta_0+h(\eta)/R=-1/a_{pp}+r_{0pp}k^2/2. \quad (64)$$

Here, δ_0 is the phase shift due to the nuclear forces in the presence of the Coulomb forces;

$$\left.\begin{aligned} &C_0^2=2\pi\eta/[\exp(2\pi\eta)-1];\quad \eta=e^2m/2\hbar^2k;\quad R=\hbar^2/me^2;\\ &h(\eta)=-\ln\eta-\gamma+\eta^2\sum_{n=1}^{\infty}\frac{1}{n(n^2+\eta^2)};\quad \gamma=0.5772;\end{aligned}\right\} \quad (65)$$

a_{pp} and r_{pp} are, respectively, the scattering length and *pp* scattering effective range.

For $k=0$ it follows that $C_0^2=0$ and $|T_{FSI}|^2=0$, i.e., when there is a final-state interaction the proton spectra have at zero relative energy, not a maximum as in the case of uncharged particles, but a minimum of the cross section.

A method of approximate allowance for the electrostatic repulsion in the case of not only a final-state interaction but also for other *pd* breakup mechanisms is given in Ref. 124.

3. INVESTIGATION OF DEFINITE REGIONS OF PHASE SPACE

In Ref. 20, data on the measurement of deuteron breakup are given Tables in 1.4.1 and 3.4.1. Our Table I augments these tables (by including later kinematically complete measurements). In the column "interpretation", we have given the authors of the computer programs used to interpret the measurements. It should however be noted that some programs exist in various variants.

Determination of the Scattering Parameters. In elementary-particle physics, the question of charge invariance and charge symmetry of the *NN* interaction has great importance. At the current time, quantitative data can be obtained by analyzing the low-energy scattering data, i.e., by comparing the scattering lengths a and effective ranges r for *S* waves in different charge states of a pair of nucleons. A review of this subject and the modern experimental values of a and r for the *pp*, *np*, and *nn* interactions, and also a bibliography can be found, for example, in Ref. 125. The review Ref. 66 is concerned with the determination of a_{nn}.

At the present time, kinematically complete measurements of deuteron breakup induced by neutrons in the *nn* final-state interaction region have given some of the most reliable determinations of a_{nn}. Careful measurements were made above all by the groups of Zeitnitz[56] and Breunlich.[55] They obtained $a_{nn}=(-16.3\pm1)F$. The values of r_{nn} are determined with large errors. More accurate measurements are as yet unavailable. In Ref. 126, Vranic *et al.* suggested that r_{nn} should be determined from quasifree *nn* scattering accompanying deuteron breakup. But this presupposes the existence of model calculations that give reliable cross sections in the QFS region.

To solve the problem of charge symmetry, it is necessary to compare a_{nn} with some *pp* scattering length a_{pp}^N with correction for the absence of electrostatic forces. However, the resulting value of a_{pp}^N depends on the adopted model, i.e., on the phase-shift-equivalent

TABLE I. Measurements of cross sections of the reactions $^2H(p,2p)n$, $H(d,2p)n$, $^2H(p,pn)p$, $^2H(n,2n)p$, $^2H(n,np)n$.

E_{lab}, MeV	θ_1, deg	θ_2, deg	$\Delta\varphi$, deg	Region of phase space	Interpretation	Reference
			$^2H(p,2p)n$			
3.8–5	θ_p^{cm}=60		180	*np* FSI excit. functions		148
7,8.5,10	30–47.7	10–62.8	180 and more	*np* QFS and FSI and more	Ebenhöh	66
8–12	θ_p^{cm}=50–80		180	*np* FSI excit. functions		46
8.5	θ_p^{cm}=41–154		180	*np* FSI ang. distrib.	EBS*	149
10,15.9,19.9	θ_p^{cm}=45–138		180	*np* FSI ang. distrib.	EBS	77
20–40	70	Accord. FSI	180	*np* FSI excit. functions	Ebenhöh	136
20–50			Measured σ_{tot}		Cahill, Sloan; KTM**	150
23	θ_p^{cm}=58–144		180	*np* FSI ang. distrib.	Ebenhöh, Haftel	37
23	50–62.8	57.8–62.8	180	Collinear case and others	Ebenhöh, Haftel	137
23,39.5	27.1–40.5	27.1–40.5	$\neq$180	Const. rel. energies	KTM; Jain, Doolen	138,139
25.8	θ_p^{cm}=44–140		180	*np* FSI ang. distrib.	EBS	140
44.9	θ_p^{cm}=60–120		180	*np* FSI ang. distrib.	Ebenhöh, Haftel	141
44.9	22–80	80–22	180 and more	*np* QFS	Ebenhöh, Haftel	81
50	34,36,38	34,36,38	140	$\lvert T_{pp}^{3/2}\rvert \approx 0$***	KTM	142
58.5	43–72	43–72	180	*np* QFS	Ebenhöh	64
			$H(d,2p)n$			
12.8	θ_p^{cm}=71–139		180	*np* FSI	EBS	140
12.9	θ_p^{cm}=72–138		180	*np* FSI	EBS	143,36
26.5			~70% of phase space		KTM	144,145
			$^2H(p,pn)p$			
6.8–11.8	19.5	30	0	*np* FSI		151
8–12	θ_p^{cm}=50–80		180	*np* FSI		46
22.1,35.7,41.1	Accord. FSI	70	180	*pp* FSI	Ebenhöh	136
			$^2H(n,2n)p$			
14.1	30	80	180	*np* FSI	Watson-Migdal	152
14.1	30,40	30,40	180	*nn* QFS	Ebenhöh	153
14.2	17.8	11	0	*nn* FSI	Ebenhöh	55
14.5	30	30,(80)	0,(180)	*nn* and *np* FSI	Cahill, Sloan	54
15.5	40	40	180	*nn* QFS		154
			$^2H(n,np)n$			
8.2–22			Measured σ_{tot}		KTM	146
14.1	0–180	0		*nn*, *np* FSI and more		147

* Ebenhöh, Bruinsma, Stuivenberg.
** Kloet, Tjon, Malfliet.
*** $\lvert T_p^{3/2}\rvert$ = *pp* quartet amplitude in Eq. (56).

potential chosen for the *NN* interaction in the *S* state to calculate the Coulomb corrections.[127,128] This explains why not only the observed three-nucleon systems but also the value of a_{pp}^N depend on the off-shell *NN* interaction. In other words, if charge symmetry is assumed, a realistic *NN* potential in the *S* state must in the absence of the Coulomb interaction reproduce the value $a_{nn}=-16.3F$ and $a_{pp}=-7.826F$ when the electrostatic forces are added. This requirement imposes certain restrictions on the off-shell interaction.

Investigations of the Region of Space with Final-State Interaction. If the kinematic conditions (see Sec. 1) are chosen in such a way that at some point on the kinematic curve the relative energy of, for example, an *np* pair is near zero, then a peak appears in the cross section due primarily to the virtual $^1S_0$ state, which is at about 67 keV (see Sec. 2). Figure 9 is an example corresponding to the same kinematic situation as Figs. 1, 2, and 6. The angle at which the proton is emitted in the center-of-mass system is called the production angle θ_p^{cm}.

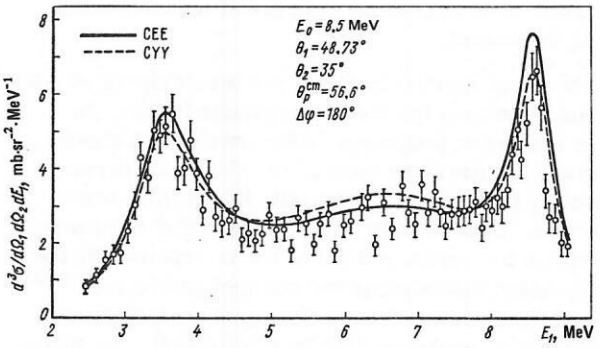

FIG. 9. Projection of *pd* breakup spectrum shown in Fig. 6 onto the kinematic curve (arc length). The two peaks correspond to the *np* FSI mechanism for the particle pairs 2–3 (E_{2-3}=38 keV) and 1–3 (E_{1-3}=0) (see Fig. 1). The curves are the result of calculation with the separable model and exponential form factor (CEE) and with the Yamaguchi form factor (CYY).

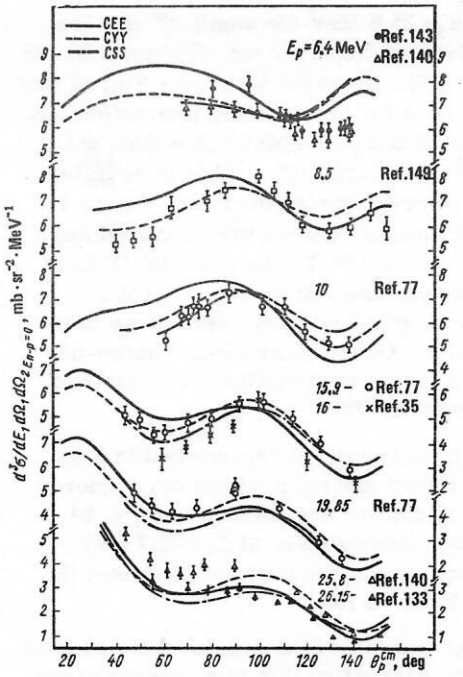

FIG. 10. Angular distributions of the $^2H(p, 2p)n$ reaction cross section for np FSI for different energies of the incident particle.

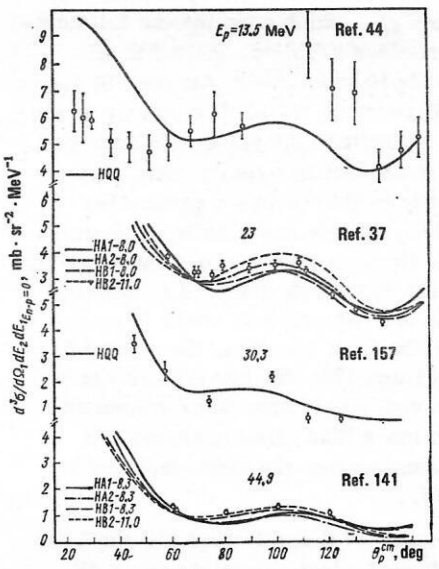

FIG. 11. Angular distributions of the $^2H(p, 2p)n$ reaction cross section for np FSI for different energies of the incident particle.

Besides making measurements for different combinations of angles, one can determine the cross section at the positions of zero relative energy of the np system as a function of the angle θ_p^{cm}. In a certain sense, this angular distribution can be ascribed to doublet scattering to a virtual level of the np system. The results of the measurements are shown in Figs. 10 and 11. The curves were calculated with the modified Ebenhöh code.[56] The abbreviation CEE means that the charge-dependent approximation (C) was used, and not the hybrid approximation (H), and the form factors of the separable potential of rank 1 in both the singlet and the triplet state have exponential form (E). A Y instead of E indicates use of the Yamaguchi potential, and S a special form factor of a separable potential of rank 2 (Fig. 13), whose off-shell behavior corresponds approximately to the Reid potential with soft core. A C at the end of the legend (for example, CEEC) means that the Coulomb interactions was taken into account in the approximation given in Ref. 132. All the curves of Fig. 11 were calculated in the hybrid approximation (H); HQQ means that form factors with quadratic dependence[56] were used. The curves HA1–8 and HB2–11 were calculated[14,37] on the basis of special potentials of rank 1 with a factor $\rho(E)$ having an explicit energy dependence. By a suitable choice of $\rho(E)$ one can generate phase-shift-equivalent potentials that lead to different triton binding energies. For HA2–8, HB2–8, and HB2–11, the same scattering parameters and phase shifts are reproduced, whereas HA1–8 gives slightly different values.[158]

Figure 12 shows the relative discrepancies between the experimental and theoretical values with and without approximate allowance for the Coulomb interaction.

Before we consider the individual distributions and the possibility of extracting information from them about the off-shell NN interaction, let us discuss this question from a general point of view. Since the FSI peak is due to the two-nucleon interaction, it may be surmised that three-particle effects are not manifested here. Indeed, the shape of the peak is determined almost completely by the enhancement factor $|T_{FSI}|^2$ (see Sec. 2). However, in the absolute cross section there

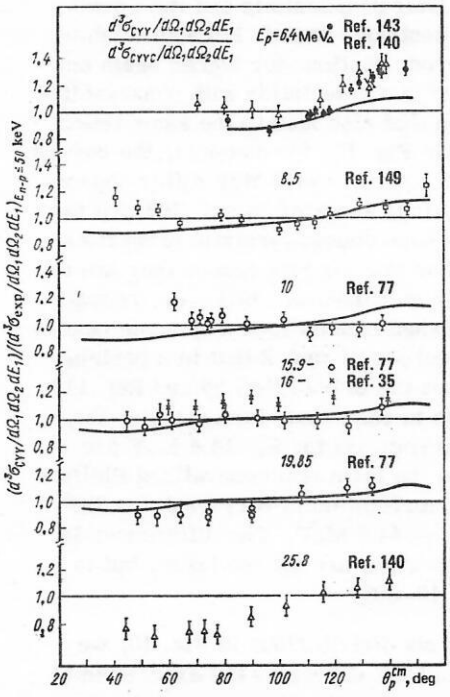

FIG. 12. Angular distributions of the cross sections shown in Fig. 10 normalized to the theoretical cross section (CYY).

is also the amplitude T_{Nd^*}, which contains the full complexity of the three-nucleon problem, including off-shell effects. Thus, there is no doubt that the FSI cross section is also sensitive to the off-shell behavior of the potential. However, two questions arise: Can one by measuring breakup cross sections really obtain new information not already contained in the properties of the bound three-nucleon system and elastic *nd* scattering, and can possible three-particle forces influence the cross section in such a way as to vitiate attempts to separate the two effects? At present, there is no unambiguous answer to the first question; the second is answered by Refs. 101 and 135: the two effects can be separated only if one considers other interactions as well or systems with more than three nucleons. In what follows, it is assumed that the three-nucleon forces can be ignored.

It has long been known[159] that different off-shell behavior for phase shift equivalent potentials gives different triton binding energies E_T and different scattering lengths of doublet elastic *nd* scattering (^2a). However, the calculated values of E_T and ^2a are correlated, and can be roughly approximated in the plot of E_T against ^2a by a straight line, the so-called Phillips line.

It was found in Ref. 55 on the basis of the boundary-condition model that the breakup cross section for $E_0 = 14.4$ MeV, $\theta_1 = \theta_2 = 47^0$, and $\varphi_1 - \varphi_2 = 159^0$ varies very little if one specifies the doublet length ^2a (or E_T). The conclusion drawn was that breakup measurements cannot yield additional information about the off-shell behavior. A special combination of angles was chosen on the basis of Ref. 11, in which particularly strong deviations were obtained at this point of phase space when the calculation was made with four different local (but not phase-shift-equivalent) potentials and the Yamaguchi potential. In contrast, in Ref. 110 appreciable differences in the cross sections for higher beam energies were obtained in a calculation with phase-shift-equivalent potentials that also lead to the same triton binding energy E_T. In Fig. 11, for example, the curves HA2–8.3 and HB2–8.3 for $E_p = 44.9$ MeV differ approximately by 10–20%. It is asserted in Ref. 108 that the employed potentials have unusual analytic properties at negative energy and that for this reason they are unsuitable for realistic calculations. However, recently Stuivenberg[13] published calculations with some phase-shift-equivalent potentials of rank 2 that in a certain sense confirm the results of both Ref. 55 and Ref. 110. Stuivenberg was able to show that, for example, the calculated FSI cross sections for $E_p = 14.4$ MeV are correlated with ^2a in the form of a generalized Phillips line. However, the correlation is very weak for 22.7 MeV and disappears at 44.9 MeV. The differences in the absolute cross sections are not too large, but in general range from 10–20%.

Examining all the six distributions in Fig. 10, we see that the potential CYY describes the experimental points somewhat better than the other potentials. In general, the deviations from the CYY curve are not greater than 10–20%. It is only for $E_p = 6.4$ MeV at large θ_p^{cm}, and at $E_p = 25.8$ MeV for small θ_p^{cm} that they exceed 20%. These deviations are not eliminated by the potentials CEE or CSS. It can be seen from Fig. 12 that approximate allowance for the Coulomb interaction improves the agreement at $E_p = 6.4$ MeV but it does not explain the deviations at large θ_p^{cm}. At other energies. a significant improvement is not observed. Figure 11 reveals similar deviations between the measured and calculated values. At 44.9 MeV, the potential HB2–11 seems somewhat preferable. However, it must be borne in mind that these calculations were made in the hybrid approximation. On the other hand, charge-dependent calculations can give deviations of more than 10% in the cross section.[160]

In addition, in the calculations represented in Figs. 10 and 11, tensor forces and the *p* waves were ignored. In the hybrid approximation, the authors of Refs. 94 and 129 showed that, for example, at $E_0 = 22.7$ MeV allowance for tensor forces and *p* waves increases the FSI cross section by up to 15%.

In conclusion, we can say of the angular distributions of the *np* final-state interaction that at an energy of the incident particle above 20 MeV one can in principle obtain new information about the *NN* interaction. For quantitative conclusions it is, however, necessary to improve the accuracy of the model calculations and also the absolute accuracy of the measurements.

For deuteron breakup induced by protons in addition to the *np* final-state interaction one can observe the *pp* final-state interaction as well, which is responsible for the appearance of the minimum in the cross section due to the electrostatic repulsion. Experimental data are given, for example, in Refs. 39 and 130–132, and the results are reviewed in Ref. 19.

The isotropy or anisotropy of the scattering in the subsystem of two nucleons with low relative energy have been analyzed on a number of occasions; for example, in Refs. 133 and 134. This question is discussed in detail in the review Ref. 19, so that we do not have to go into it further here.

Investigations of Quasifree Scattering. Up to 1975, a large number of investigations had been published on both *np* and *pp* quasifree scattering. The results of the measurements are presented in Table 4 of the review Ref. 19. The experimental investigations include measurements of the QFS peaks as a function of the cms production angle, i.e., the QFS angular distributions, at different beam energies, as well as measurements of the QFS peaks for symmetric coplanar angles as a function of the energy of the incident particle. As an example, Fig. 13 shows the angular distributions of the cross sections in the laboratory system at $E_0 = 23$ MeV.[162] The plotted curves were calculated in accordance with Ebenhöh's code using the Yamaguchi potential in the hybrid approximation. For *np* scattering, the departure from the experimental values is ~10–20%; for the *pp* cross sections at small and large angles there are large discrepancies, these being obviously due to the neglect of the Coulomb interaction. The difference between the absolute cross sections at the *np* and *pp*

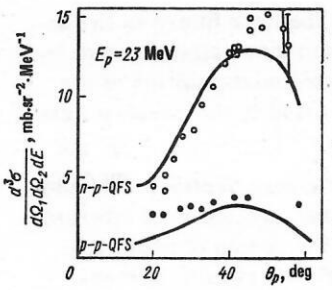

FIG. 13. Angular distribution of *np* (open circles) and *pp* (black circles) cross sections in the laboratory system for quasifree scattering.

peaks is a consequence of the Pauli principle.

Compared with theoretical calculations for the FSI case, the calculated absolute values of the QFS cross section depend more strongly on the on-shell potentials that are used. For example, at $E_0 = 23$ and 45 MeV Refs. 100 and 81) the potentials give a small difference in the phase shifts and an appreciable difference (~35%) in the QFS cross section. But phase-shift-equivalent potentials lead to almost unchanged QFS cross sections. This result shows that the QFS cross sections are insensitive to the off-shell behavior.

A characteristic of the calculated QFS cross sections is that the partial wave of total orbital angular momentum with $L = 0$ does not make the dominant contribution to the total cross section, other partial waves being added coherently. This partly explains the insensitivity of the cross section to the off-shell potential since only the term of the doublet amplitude [see (56)] with $L = 0$, i.e., states in which all three nucleons are simultaneously at short distances from one another, is sensitive to the off-shell behavior.

Another characteristic result of the QFS calculations is that for not too high energies of the incident particle there is strong destructive interference between definite terms of (56). To a large extent, it determines not only the absolute value but also the shape of the QFS peak. This is one of the important reasons why the approximate methods mentioned in Sec. 2–the simple impulse approximation and its modifications–give overestimated absolute values of the QFS peak. It is only at beam energy above 70 MeV for *np* quasifree scattering and above 120 MeV for *pp* quasifree scattering that these methods give absolute values in approximate agreement with the experimental data.

At higher energies of the incident particle, the angular distributions of the cross sections of *pp* quasifree scattering calculated in accordance with Ebenhöh's code agree better with the experiments. For example, the angular distribution of *pp* quasifree scattering constructed on the basis of the measurements of Ref. 163 at $E_0 = 65$ MeV is better described by the theoretical curves than the distribution at $E_0 = 23$ MeV shown in Fig. 13. This is one more indication that the deviations are due to the neglect of the Coulomb interaction.

In Ref. 13, Stuivenberg made charge-dependent calculations in accordance with the EBS program for the QFS region as well for phase-shift-equivalent potentials of rank 2. He confirmed that the changes in the cross section at $E_0 = 22.7$ and 44.9 MeV are less than 2%, while at $E_0 = 14.4$ MeV they reach 10%. However, as in the FSI case, at low energy there is a fairly strong correlation between the QFS cross section and the doublet scattering length ^2a obtained for the considered potentials.

In Ref. 94, the influence of *p* waves and tensor forces on the cross section and polarization for the QFS case was considered. The calculations are not charge dependent and were made for the reaction ^{2}H$(n, 2n)p$. It was found that the changes in the QFS cross section at 23 MeV are 15%.

Investigation of the Region of Phase Space with Two Equal and Constant Relative Energies; the Collinear Case. With the aim of finding a region more sensitive to the off-shell behavior of the interaction, there have been investigations in recent years of the part of the phase space in which the relative energies between the pairs are not only constant but also equal.[164, 11, 165, 138, 13, 129] A guiding argument here is that all points of the region of phase space with constant relative energies the two-particle effects must occur in approximately the same way. This must facilitate the study of the genuine three-particle effects. In this case, the term $T_3^{1/2}$, which depends strongly on the dynamics of the process, will be predominant in (56). If moreover symmetric angles are chosen, it then follows from symmetry considerations (three equal relative energies) that only this single term remains.[138] Because of the destructive interference of the Born term with the remainder (the contribution of multiple scattering) a minimum appears in $T_3^{1/2}$, and its position and depth depend sensitively on the relative energy and on the potential, in particular, on its off-shell properties.[13]

In Fig. 14, the result of measurement[165] for two equal and constant relative energies is compared with the calculations for three different potentials. Although

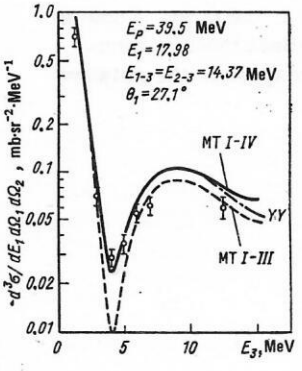

FIG. 14. Cross section of the reaction ^{2}H$(p, 2n)n$ for two equal and constant relative energies. The measurements are taken from Ref. 138. The curves are the result of calculations made with the Malfliet—Tjon program[167] with local potentials MTI-IV and MTI-III and in accordance with the program of Ref. 168 with Yamaguchi potentials (YY).

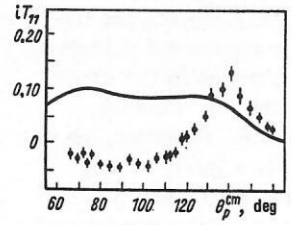

FIG. 15. Vector analyzing power iT_{11} for np FSI.

the potential MTI-III reproduces the phase shifts up to 300 MeV and the triton binding energy well, the cross section at the minimum is only one third of the measured value. Allowance for p waves, tensor forces,[129] or an 8% D admixture in the deuteron[165] makes it possible to obtain a shallower minimum. It should be noted in this connection that the strong dependence on the p-wave intensity, the tensor forces, and the D admixture strongly restricts the possibility of extracting information about the off-shell behavior.

An investigation has also been made of the collinear case (see Sec. 2), when the relative energies of two particles are equal and the third is at rest in the common center-of-mass system.[137] The theoretical investigations[13] show that the deviations due to the different off-shell behavior reach 50%. In contrast to other regions of phase space, the quartet amplitude is here dominant.

Results of Polarization Measurements. As we have noted in Sec. 2, few measurements have yet been made of polarization in deuteron breakup. Model calculations were made in Ref. 94. The interaction in all four P states and tensor forces were taken into account but the Coulomb interaction and charge dependence were not. The calculated vector analyzing power iT_{11} for np final-state interaction at $E_0 = 22.7$ MeV for the reaction $n(d, 2n)p$ is compared with the measurements[92] of this parameter for the reaction $H(d, 2p)n$ at $E_d = 45.4$ MeV.[165] The result is shown in Fig. 15. The curve is calculated on the basis of the Yamaguchi form factors for the states $^1S_0$ and $^3S_1 - {}^3D_1$ with a 7% D admixture and with the p-wave interaction introduced in Ref. 92 for calculation of elastic scattering. A strong discrepancy between the calculated curve and the experimental data is observed; the reason for this is unknown. Some of the deviations may be due to the fact that the measurements are integrated with respect to the relative energy in the interval 0–1 MeV.

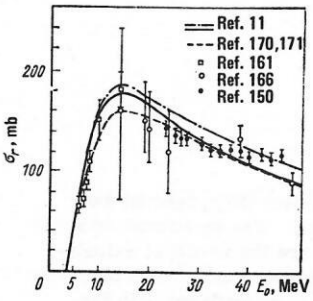

FIG. 16. Total cross section of deuteron breakup reaction.

It is to be expected that in the near future in the investigation of deuteron breakup more attention will be devoted to polarization. A detailed exposition of the situation in this area can be found in the reviews Refs. 174 and 173.

Measurements of the Total Cross Section. The energy dependence of the total cross section is of interest for various applications. In the region of projectile nucleon energies up to 50 MeV the results of measurements of the total cross section of the $n + {}^2H$ breakup reaction are given in Refs. 161 and 166, and for the reaction $p + {}^2H$ in Ref. 150 (Fig. 16). The curves are calculated for the reaction $n + {}^2H$ in Refs. 170 and 171 for separable potentials and in Ref. 11 for local potentials. The curves satisfactorily describe the experimental points. Although the measurements of Ref. 150 were made for reactions with protons, they agree well with other measurements and with the theoretical curves. It is obvious that at $E_0 = 20$ MeV the influence of the Coulomb interaction can be ignored.

CONCLUSIONS

The main aim of Nd breakup investigations is to obtain information about the off-shell behavior of the nuclear forces and also the role of three-particle forces. As is shown in Ref. 101, this problem is made much harder by the basic impossibility of separating the two effects even if all three-particle data (elastic scattering, inelastic scattering in the whole of the phase space, and polarization parameters) were known exactly from the experiments. To separate the off-shell properties and the three-particle forces it is necessary to investigate either a property of systems with more than three nucleons or the scattering of particles with an electromagnetic or weak interaction in the three-nucleon system. At the present time, the three-nucleon system is investigated in the first place by means of phase-shift-equivalent potentials. The changes in the calculated three-particle quantities when the off-shell behavior is varied are studied. In the same manner, one can also study the sensitivity to the three-particle forces. In the case of a bound state of three nucleons, the binding energy is changed by about 1–2 MeV as a result of variation of the off-shell behavior and by 2–3 MeV as a result of variation of the three-particle forces. For Nd breakup, systematic investigations have not yet been made of the spectra in their dependence on the three-particle forces. Systematic investigations into the dependence of the spectra on the off-shell behavior have been made in the last three years. Before this, potentials that describe the two-nucleon data only at low energy were mainly used.

The existing studies have revealed roughly a 30% dependence of the breakup cross sections on the off-shell behavior. The results of theory agree with about the same accuracy with the experiments. The experimental uncertainties of modern measurements of Nd breakup are 5–10%.

At the present time it is still impossible to extract quantitative data about off-shell effects and three-par-

ticle forces from experiments. To achieve this aim, it is necessary to go over from the currently used separable S-wave potentials to a realistic interaction with allowance for higher partial waves and tensor forces. Further, it is necessary to develop practical methods for taking into account the Coulomb interaction. The implementation of such calculations in the framework of the Faddeev equations requires much time and a large computer memory. This leads to long and expensive investigations. Therefore, one of the important tasks of subsequent studies of Nd breakup will be to develop mathematical methods of more effective solutions of the Faddeev integral equations. It may be that a formulation of the scattering equations more suitable for numerical calculations can be found.

An important question in connection with study of the off-shell behavior is the parametrization of the dependence of the three-particle quantities on the off-shell properties. The existing theoretical investigations indicate that the off-shell behavior at low energies (up to about 20 MeV) can be characterized by a single parameter, the doublet scattering length ^2a usually being chosen. The generalized Phillips line expresses the approximate monotonic dependence of the Nd cross section at a certain point of phase space on ^2a. This phenomenon is analogous to the well known Phillips line, which represent the binding energy E_T of the three-nucleon system as a function of the doublet length ^2a. At energies above 20 MeV, it is no longer possible to parametrize the off-shell behavior by a single parameter.

Despite the unresolved problems that we have mentioned, it must be said that the investigations hitherto made into Nd breakup have led to important results.

Experiments on Nd breakup with complete kinematics have been made during the last ten years. It has been established that measurements of this kind make it possible to determine the two-nucleon scattering parameters with good accuracy. It was first shown that the np and pp scattering lengths determined from Nd breakup agree with the corresponding free scattering lengths. Then on the basis of these results, the nn scattering length was measured. There followed detailed investigations of the reaction mechanisms in three-particle reactions. It was found that final-state interaction and quasi-free scattering are the dominant mechanisms. Experiments on Nd breakup fostered the practical development of the theory of a three-body quantum-mechanical system. It should be emphasized that a three-particle system is a kind of bridge between a two-particle system and many-particle systems. On the one hand it is sufficiently simple to admit rigorous calculations (at the present time, for relatively simple potentials). But, on the other, it enables one, for example, to study scattering processes with rearrangement of the particles, i.e., phenomena characteristic of many-particle problems. In particular, investigations have also been made of questions such as the representation of the two-particle potential and the two-particle scattering matrix in separable form, the unitarity of separable expansions, the convergence and analytic properties of the multiple Nd scattering series, and the development of numerical methods of solution of singular integral equations.

It bears noting that the description of the three-nucleon system does not contain free parameters. This is a rare case in nuclear physics.

The comparison between theory and experiment shows that both the structure and absolute value of the breakup spectra are described remarkably well even if the two-particle interaction is taken in the form of a separable potential that correctly reproduces the two-particle data only at low energy. In the language of the analytic properties of the T matrix this result means that the breakup spectra are basically determined by the unitary two-particle and three-particle cuts and the two poles corresponding to the $^1S_0$ and $^3S_1$ states in the two-particle amplitude.

Calculations of the breakup spectra using local potentials have led to an interesting application of the method of Padé approximation. In addition, they have shown that in general the spectra change little if separable potentials are used instead of local potentials.

As we have already said, many unsolved theoretical problems remain. It seems to us that further experimental investigations will be basically directed toward improving the existing measurements, to studying further regions of the phase space, and to measurement of the effective range of the nn interaction. In addition, it is to be expected that the main thrust of Nd breakup experiments will be shifted to experiments with polarized particles.

[1]L. D. Faddeev, Zh. Éksp. Teor. Fiz. **39**, 1459 (1960) [Sov. Phys. JETP **12**, 1014 (1961)].
[2]A. N. Mitra, Nucl. Phys. A **32**, 529 (1962).
[3]R. D. Amado, Phys. Rev. **132**, 485 (1963).
[4]C. Lovelace, Phys. Rev. **135**, B1225 (1964).
[5]A. G. Sitenko and V. F. Kharchenko, Nucl. Phys. **49**, 15 (1963).
[6]S. Weinberg, Phys. Rev. **131**, 440 (1963); Phys. Rev. **130**, 776 (1963).
[7]E. O. Alt, P. Grassberger, and W. Sandhas, Nucl. Phys. B **2**, 167 (1967).
[8]R. I. Cahill and I. H. Sloan, Nucl. Phys. A **165**, 161 (1971).
[9]E. Ebenhöh, Nucl. Phys. A **191**, 97 (1972).
[10]W. M. Kloet and J. A. Tjon, Ann. Phys. **79**, 407 (1973).
[11]W. M. Kloet and J. A. Tjon, Nucl. Phys. A **210**, 380 (1973).
[12]M. I. Haftel and E. L. Petersen, Phys. Rev. Lett. **33**, 1229 (1974).
[13]J. H. Stuivenberg, Thesis, Amsterdam, Vrije Universiteit (1976).
[14]A. N. Mitra, Adv. Nucl. Phys. **3**, 1 (1969).
[15]A. G. Sitenko and V. F. Kharchenko, Usp. Fiz. Nauk **103**, 469 (1971) [Sov. Phys. Usp. **14**, 125 (1971)].
[16]Y. E. Kim and A. Tubis. Ann. Rev. Nucl. Sci. **24**, 69 (1974).
[17]E. W. Schmidt and H. Ziegelmann, The Quantum Mechanical Three-Body Problem, Vieweg, Braunschweig, 1974; Pergamon, 1974.
[18]J. S. Levinger, Springer Tracts Mod. Phys. **71**, 88 (1974).
[19]W. Kluge, Fortschr. Phys. **22**, 691 (1971).
[20]S. Fiarman and S. S. Hanna, Nucl. Phys. A **251**, 1 (1975).
[21]M. Durand, Z. Phys. A **275**, 397 (1975).
[22]I. Slaus, In: Proc. Conf. on Few Particle Problems, Los Angeles, North-Holland, Amsterdam (1972), p. 272.

[23]H. G. Pugh, In: Proc. Conf. on Few Body Dynamics, Delhi, North-Holland, Amsterdam (1976), p. 625.
[24]B. Kühn, Fiz. Élem. Chastits At. Yadra 6, 347 (1975) [Sov. J. Part. Nucl. 6, 139 (1975)].
[25]G. G. Ohlsen, Nucl. Instrum. Methods 37, 240 (1965).
[26]R. H. Dalitz, Philos. Mag. 44, 1068 (1953).
[27]H. Brückmann, W. Kluge, and L. Schänzler, Z. Phys. 217, 350 (1968).
[28]B. Kühn *et al.*, Nucl. Phys. A 120, 285 (1968).
[29]D. P. Boyd, P. F. Donovan, and H. F. Mollenauer, Phys. Rev. 188, 1544 (1969).
[30]A. Niiler *et al.*, Phys. Rev. 182, 1083 (1969).
[31]J. D. Margaziotis *et al.*, Phys. Rev. C 2, 2050 (1970).
[32]B. Sundqvist *et al.*, Report TLU 4/72, Uppsala (1972).
[33]J. L. Durand *et al.*, Phys. Rev. C 6, 393 (1972).
[34]D. L. Shannon, Thesis UCLA (1973).
[35]H. Klein *et al.*, Nucl. Phys. A 199, 169 (1973).
[36]G. D. Thijs, P. H. Schram, and C. C. Jonker, Nucl. Phys. A 205, 413 (1973).
[37]E. L. Petersen *et al.*, in: Proc. Conf. on Few Body Problems, Quebec, North-Holland, Amsterdam (1974), p. 395.
[38]R. Fülle *et al.*, Exptl. Techn. Phys. 23, 245 (1975).
[39]M. Ivanovich *et al.*, Nucl. Phys. A 156, 616 (1970).
[40]J. C. van der Weerd *et al.*, Phys. Rev. C 3, 66 (1971).
[41]W. J. Braithwaite *et al.*, Nucl. Phys. A 166, 515 (1971).
[42]V. Valković *et al.*, Nucl. Phys. A 166, 547 (1971).
[43]E. Andrade *et al.*, Nucl. Phys. A 183, 145 (1972).
[44]J. P. Burq *et al.*, Nucl. Phys. A 179, 371 (1972).
[45]J. Kecskeméti and T. Czibók, Phys. Rev. Lett. 32, 1063 (1974).
[46]R. Plasek, V. Valkorić, and G. C. Phillips, Nucl. Phys. A 256, 189 (1976).
[47]E. Graf *et al.*, Helv. Phys. Acta 39, 578 (1966).
[48]R. Honecker and H. Grässler, Nucl. Phys. A 107, 81 (1968).
[49]H. Grässler and R. Honecker, Nucl. Phys. A 136, 446 (1969).
[50]B. Zeitnitz, R. Maschuw, and P. Suhr, Nucl. Phys. A 149, 449 (1970).
[51]Dropmann, Thesis, Aachen (1971).
[52]I. Slaus *et al.*, Phys. Rev. Lett. 26, 789 (1971).
[53]M. W. McMaughton *et al.*, in: Proc. Conf. on Few Body Problems, Los Angeles, North-Holland, Amsterdam (1972), p. 108.
[54]R. Bouchez *et al.*, Nucl. Phys. A 185, 166 (1972).
[55]W. H. Breunlich *et al.*, Nucl. Phys. A 221, 269 (1974).
[56]B. Zeitnitz *et al.*, Nucl. Phys. A 231, 13 (1974).
[57]S. Matsuki, M. Yasue, and S. Yamashita, Nucl. Instrum. Methods 94, 387 (1971).
[58]B. Sundqvist *et al.*, Report TLU 14/73, Uppsala (1973).
[59]G. Heintze and J. Mösner, Annual Report ZfK-283 (1974), p. 150.
[60]B. Sundqvist *et al.*, Report TLU 15/73, Uppsala (1973).
[61]B. Sundqvist *et al.*, Annual Report TLU 75, Uppsala (1975), p. 17.
[62]F. S. Goulding and B. G. Harvey, Ann. Rev. Nucl. Sci. 25, 167 (1975).
[63]G. Anzelon *et al.*, Nucl. Phys. A 202, 593 (1973).
[64]J. L. Durand *et al.*, Nucl. Phys. A 224, 77 (1974).
[65]H. Brückmann *et al.*, Nucl. Instrum. Methods 67, 29 (1969).
[66]B. Kühn *et al.*, Nucl. Phys. A 247, 21 (1975).
[67]R. G. Allas, in: Proc. Conf. on Few Body Dynamics, Delhi, North-Holland Amsterdam (1976), p. 455.
[68]L. A. C. Koerts *et al.*, Nucl. Instrum. Methods 92, 157 (1971).
[69]D. P. Saylor, Nucl. Instrum. Methods 94, 253 (1971).
[70]B. Sundqvist *et al.*, Annual Report TLU, Uppsala (1975).
[71]J. Arvieux *et al.*, Nucl. Phys. A 150, 75 (1970).
[72]F. N. Rad *et al.*, Phys. Rev. Lett. 31, 57 (1973); 33, 1227 (1974); 35, 1134 (1975); Phys. Rev. C 8, 1248 (1973).
[73]C. O. Blyth *et al.*, in: Proc. Conf. on Few Body Problems, Quebec, North-Holland, Amsterdam (1974), p. 597; Walter *et al.*, *ibid.* p. 587.
[74]F. Gabriel, Thesis, Report ZfK-228 (1972).
[75]E. D. Cashwell and C. J. Everett, A Practical Manual on the Monte Carlo Method for Random Walk Problems, Pergamon Press, Amsterdam (1959).
[76]L. Glantz and I. Koersner, Annual Report TLU, Uppsala (1975), p. 19.
[77]W. Krijgsman, Thesis, Vrije Universiteit, Amsterdam (1976).
[78]J. A. Schreider, Method of Statistical Testing, Elsevier (1964).
[79]M. L. Goldberger and K. M. Watson, Collision Theory, Sec. 3. Wiley, New York (1964).
[80]M. I. Haftel, Phys. Rev. C 7, 80 (1973).
[81]M. I. Haftel *et al.*, Nucl. Phys. A 269, 359 (1976).
[82]M. A. Preston, Physics of the Nucleus, Addison-Wesley, Reading, Mass. (1962) (Russian translation, Mir, Moscow (1964), p. 552).
[83]H. P. Noyes, in: Proc. Conf. Brela (1967), p. 10.
[84]L. D. Faddeev, Tr. Mat. Inst. Akad. Nauk SSSR 69 (1963).
[85]S. Weinberg, Phys. Rev. 133, B232 (1964).
[86]R. L. Omnes, Phys. Rev. 134, B1358 (1964).
[87]A. Ahmadzadeh and J. A. Tjon, Phys. Rev. 139, B1085 (1965).
[88]R. Balian and E. Brézin, Nuovo Cimento B 61, 403 (1969).
[89]E. Elbaz *et al.*, Acta Physiol. Acad. Aci. Hung. 33, 243 (1973).
[90]T. A. Osborn, Report SLAC 1967, Humbertson.
[91]H. Ziegelmann, Nucl. Phys. A 192, 426 (1972).
[92]P. Doleschall, Nucl. Phys. A 201, 264 (1973).
[93]S. C. Pieper, Phys. Rev. C 8, 1702 (1973).
[94]J. Bruinsma and R. Van Wageningen, Phys. Lett. B 63, 19 (1976).
[95]R. Aaron, R. D. Amado, and Y. Y. Yam, Phys. Rev. 140, B1291 (1965); 150, 857 (1966).
[96]J. H. Hetherington and L. H. Schink, Phys. Rev. 137, B935 (1965).
[97]F. Sohre and H. Ziegelmann, Phys. Lett. B 34, 579 (1971).
[98]M. G. Fuda, Phys. Rev. Lett. 32, 620 (1974).
[99]V. B. Belyaev and K. Möller, Report JINR E4-9911, Dubna (1976).
[100]E. L. Petersen *et al.*, Phys. Rev. C 9, 508 (1974).
[101]H. P. Noyes, Phys. Rev. Lett. 23, 1201 (1969).
[102]S. P. Merkur'ev, Teor. Mat. Fiz. 8, 235 (1971).
[103]S. P. Merkuriev, Nucl. Phys. A 233, 395 (1974).
[104]A. Laverne and G. Gignoux, Nucl. Phys. A 203, 597 (1973).
[105]G. Gignoux and A. Laverne, Phys. Rev. Lett. 33, 1350 (1974).
[106]D. D. Brayshaw, Phys. Rev. D 8, 952 (1973).
[107]Y. E. Kim and A. Tubis, Phys. Lett. B 38, 354 (1972).
[108]D. D. Brayshaw, Phys. Rev. Lett. 32, 382 (1974); 34, 1478 (1975).
[109]V. N. Efimov and H. Schulz, Nucl. Phys. A 261, 328 (1976).
[110]M. I. Haftel and E. L. Petersen, Phys. Rev. Lett. 34, 1480 (1975).
[111]D. D. Brayshaw, Phys. Rev. C 13, 1835 (1976).
[112]K. M. Watson, Phys. Rev. 88, 1163 (1952).
[113]A. B. Migdal, Zh. Éksp. Teor. Fiz. 28, 3 (1955) [Sov. Phys. JETP 1, 2 (1955)].
[114]G. F. Chew and F. E. Low, Phys. Rev. 113, 1640 (1959).
[115]A. F. Kuckes, R. Wilson, and P. F. Cooper, Jr., Ann. Phys. (N. Y.) 15, 193 (1961).
[116]G. Paic, J. C. Young, and D. J. Margaziotis, Phys. Lett. B 32, 437 (1970).
[117]J. A. McIntyre *et al.*, Phys. Rev. C 5, 1796 (1972).
[118]P. U. Sauer, in: Proc. Conf. on Few Body Dynamics, Delhi, North-Holland, Amsterdam (1976), p. 488.
[119]A. M. Veselova, Teor. Mat. Fiz. 3, 326 (1970); 13, 368 (1972).
[120]G. Bencze, Nucl. Phys. A 196, 135 (1972).
[121]S. P. Merkur'ev, Yad. Fiz. 24, 289 (1976) [Sov. J. Nucl. Phys. 24, 150 (1976)].
[122]E. O. Alt *et al.*, Phys. Rev. Lett. 37, 1537 (1976).
[123]H. Matthäu and H. D. Zeh, Report KfK-1547 (1972); Nucl. Phys. A 192, 39 (1972).

[124]W. Ebenhöh, Report, Universität Heidelberg (1973).
[125]J. I. De Swart, in: Proc. Conf. on Few Body Problems, Quebec, North-Holland, Amsterdam (1974), p. 235.
[126]D. Vranic *et al.*, in: Proc. Conf. on Few Body Problems, Quebec, North-Holland, Amsterdam (1974), p. 660.
[127]H. Kumpf, Yad. Fiz. **17**, 1156 (1973) [Sov. J. Nucl. Phys. **17**, 602 (1973)].
[128]P. U. Sauer, Phys. Rev. Lett. **32**, 626 (1974).
[129]J. Bruinsma, Thesis, Vrije Universiteit, Amsterdam (1976).
[130]H. Brückmann *et al.*, Report KfK-1012, Karlsruhe (1969); Phys. Lett. B 30, 460 (1969).
[131]J. G. Rogers, M. Jain, and J. D. Bronson, Phys. Rev. C 8, 961 (1973).
[132]W. Ebenhöh *et al.*, Report TLU 23/73, Uppsala (1973).
[133]H. Brückmann *et al.*, Nucl. Phys. A **157**, 209 (1970).
[134]B. J. Wielinga *et al.*, in: Proc. Conf. on Few Body Problems, Los Angeles, North-Holland, Amsterdam (1972).
[135]D. D. Brayshaw, Phys. Rev. C **13**, 1024 (1976).
[136]D. Bonbright, J. W. Watson, and D. J. Roberts, in: Proc. Conf. on Few Body Problems, Quebec, North-Holland, Amsterdam (1974), p. 420.
[137]J. M. Lambert *et al.*, Phys. Rev. C **13**, 43 (1976).
[138]W. T. H. Van Oers, in: Proc. Conf. on Few Body Dynamics, Delhi, North-Holland, Amsterdam (1976), p. 746.
[139]A. M. McDonald *et al.*, Phys. Rev. Lett. **34**, 488 (1975).
[140]J. Doornbos, Thesis, Vrije Universiteit, Amsterdam (1977).
[141]E. L. Petersen *et al.*, in: Proc. Conf. on Few Body Dynamics, Delhi, North-Holland, Amsterdam (1976), p. 201.
[142]G. J. F. Blommestijn, *Ibid.* p. 212.
[143]P. H. Schram, Thesis, Vrije Universiteit, Amsterdam (1975).
[144]B. J. Wielinga *et al.*, Nucl. Phys. A **261**, 13 (1976).
[145]R. Van Dantzig *et al.*, in: Proc. Conf. on Few Body Dynamics, Delhi, North-Holland, Amsterdam (1976), p. 209.
[146]G. Pauletta and F. D. Brooks, Nucl. Phys. A **225**, 267 (1975).
[147]J. Kecskéméti and T. Czibók, Phys. Rev. Lett. **32**, 1063 (1974).
[148]S. Matsuki *et al.*, in: Proc. Conf. on Few Body Problems, Los Angeles, North-Holland, Amsterdam (1972), p. 535.
[149]G. Schmidt, Private Communication.
[150]R. F. Carlsson *et al.*, in: Proc. Conf. on Few Body Problems, Los Angeles, North-Holland, Amsterdam (1972), p. 475.
[151]F. Cocu, G. Ambrosino, and D. Guerreau, *ibid.* Quebec, North-Holland, Amsterdam (1974), p. 662.
[152]C. Lunke, J. P. Egger, and J. Rossel, Nucl. Phys. A **158**, 278 (1970).
[153]E. Bovet, F. Foroughi, and J. Rossel, Helv. Phys. Acta **48**, 137 (1975).
[154]L. P. Dryapachenko *et al.*, Nucl. Instrum. Methods **141**, 153 (1977).
[155]N. M. Smirnov and I. W. Dunin-Barkowski, Mathematische Statistik in der Technik, VEB Deutscher Verlag der Wissenschaften, Berlin (1963), p. 238.
[156]J. Bruinsma *et al.*, Nucl. Phys. A **228**, 52 (1974).
[157]D. J. Margaziotis *et al.*, Phys. Rev. C 8, 870 (1973).
[158]M. I. Haftel, E. L. Petersen, and J. M. Wallace, Phys. Rev. C **14**, 419 (1976).
[159]A. C. Phillips, Nucl. Phys. A **107**, 209 (1968).
[160]J. H. Stuivenberg, J. Bruinsma, and R. Van Wageningen, in: Proc. Conf. on Few Body Problems, Quebec, North-Holland, Amsterdam (1974), p. 505.
[161]H. C. Catron *et al.*, Phys. Rev. **123**, 218 (1961).
[162]E. L. Petersen *et al.*, in: Proc. Conf. on Few Body Problems, Los Angeles, North-Holland, Amsterdam (1972), p. 503.
[163]V. K. C. Cheng and P. G. Roos, Nucl. Phys. A **225**, 397 (1974).
[164]M. Jain, J. G. Rogers, and D. P. Saylor, Phys. Rev. Lett. **31**, 838 (1973).
[165]A. M. McDonald *et al.*, Phys. Rev. Lett. **34**, 488 (1975).
[166]J. D. Seagrave *et al.*, LA 52 Report LA-DC-12954.
[167]R. A. Malfliet and J. A. Tjon, Nucl. Phys. A **127**, 161 (1969).
[168]M. Jain and G. D. Doolen, Phys. Rev. C 8, 124 (1973).
[169]F. N. Rad *et al.*, Phys. Rev. Lett. **35**, 1134 (1975).
[170]R. T. Cahill and I. H. Sloan, Nucl. Phys. A **165**, 161 (1971).
[171]I. H. Sloan, Nucl. Phys. A **168**, 211 (1971).
[172]D. Kamke, Ann. Phys. (N. Y.) **28**, 193 (1972).
[173]H. E. Conzett, in: Proc. Conf. on Few Body Dynamics, Delhi, North-Holland, Amsterdam (1976), p. 611.
[174]H. E. Conzett, in: Proc. Conf. on Few Body Problems, Quebec, North-Holland, Amsterdam (1974), p. 566.

Translated by Julian B. Barbour